Special Issue: Earthquake geology

Seismic intensity assignments for the 2008 Andravida (NW Peloponnese, Greece) strike-slip event (June 8, Mw=6.4) based on the application of the Environmental Seismic Intensity scale (ESI 2007) and the European Macroseismic scale (EMS-98). Geological structure, active tectonics, earthquake environmental effects and damage pattern

Spyridon D. Mavroulis[1,*], Ioannis G. Fountoulis[1], Emmanuel N. Skourtsos[1], Efthymis L. Lekkas[1], Ioannis D. Papanikolaou[2]

[1] *National and Kapodistrian University of Athens, Faculty of Geology and Geoenvironment, Department of Dynamic Tectonic Applied Geology, Panepistimiopolis, Athens, Greece*

[2] *Agricultural University of Athens, Department of Geological Sciences and Atmospheric Environment, Laboratory of Mineralogy and Geology, Athens, Greece*

Article history
Received October 19, 2012; accepted November 14, 2013.
Subject classification:
Active faults, Earthquake environmental effects, ESI 2007 intensity scale, EMS-98 intensity scale, Strike-slip earthquakes.

ABSTRACT

On June 8, 2008, a strike-slip earthquake (Mw=6.4) was generated NE of the Andravida town (NW Peloponnese, western Greece) due to the activation of the previously unknown western Achaia strike-slip fault zone (WAFZ). Extensive structural damage and earthquake environmental effects (EEE) were induced in the NW Peloponnese, offering the opportunity to test and compare the ESI 2007 and the EMS-98 intensity scales in a moderate strike-slip event. No primary EEE were induced, while secondary EEE including seismic fractures, liquefaction phenomena, slope movements and hydrological anomalies were widely observed covering an area of about 800 km^2. The lack of primary effects and the relatively small surface deformation with respect to the earthquake magnitude is due to the thick Gavrovo flysch layer in the affected area that isolated and absorbed the subsurface deformation from the surface. According to the application of the EMS-98 scale, damage to masonry buildings ranged from grade 3 to 5, while damage in most of R/C buildings ranged from grade 1 to 3. A maximum ESI 2007 intensity VIII-IX is recorded, while the maximum EMS-98 intensity is IX. For all the sites where intensity VIII has been recorded the ESI 2007 and the EMS-98 agree, but for others the ESI 2007 intensities values are lower by one or two degrees than the corresponding EMS-98 ones, as it is clearly concluded from the comparison of the produced isoseismals. An exception to this rule is the Valmi village, where considerable structural damage occurs (IX_{EMS-98}) along with the lack of significant EEE ($V_{ESI\ 2007}$). This variability between the ESI 2007 and the EMS-98 intensity values is predominantly attributed to the vulnerability of old masonry buildings constructed with no seismic resistance design. Correlation of all existing data shows that the geological structure, the active tectonics, and the geotechnical characteristics of the alpine and post-alpine formations along with the construction type of buildings were of decisive importance in the damage and the EEE distribution.

1. Introduction

Earthquake environmental effects (EEE) have been increasingly disregarded in the literature and the practice of macroseismic investigations during the 20th century, while increasing attention has been directed towards the analysis of the effects on humans and manmade structures. The European Macroseismic scale (EMS-98), which is predominantly used in Europe, considers three categories of effects: (a) on humans, (b) on objects and on nature and (c) damage to buildings [Grünthal 1998]. Its basic advantage over previous macroseismic intensity scales is a definition of vulnerability classes for buildings and more precise statistical treatment of collected macroseismic data [Grünthal 1998]. This quantification is elaborated in details for the effects on humans, objects and buildings, but not for the effects on nature which are rather briefly summarized in a table in EMS-98 scale. This allows a large discrepancy between the EEE and the damage pattern.

Recent studies [Dengler and McPherson 1993, Serva 1994, Dowrick 1996, Esposito et al. 1997, Hancox et al. 2002, Michetti et al. 2004, 2007, Castilla and Audemard 2007, Serva et al. 2007, Silva et al. 2008, Reicherter et al. 2009, Gosar 2012] offered new substantial evidence that coseismic environmental effects provide valuable information on the earthquake size and its intensity field, complementing the traditional damage-based macroseismic scales. Indeed, with the outstanding growth of paleoseismology and earthquake geology, nowadays the effects on the environment can be described and quantified with a remarkable detail compared with that available at the time of the earlier scales. Therefore, today the definition of the intensity degrees can effectively take advantage of the diagnostic characteristics of the effects on natural environment.

Earthquake environmental effects (EEE) are any effect produced by a seismic event on natural environment [Michetti et al. 2007]. Several decades of research on earthquake geology and paleoseismology have pointed out their crucial role in seismic hazard assessment, due to their relations with the earthquake size and the location of seismogenic sources [Dengler and McPherson 1993, Serva 1994, Wells and Coppersmith 1994, Esposito et al. 1997]. The coseismic environmental effects considered diagnostic for intensity evaluation can be categorized in two main types [Michetti et al. 2007]: (a) Primary effects, which are directly linked to the earthquake energy and in particular to the surface expression of the seismogenic source, including surface faulting, surface uplift and subsidence and any other surface evidence of coseismic tectonic deformation; (b) Secondary effects including phenomena generally induced by the ground shaking. They are conveniently classified into eight main categories that are hydrological anomalies, anomalous waves including tsunamis, ground cracks, slope movements, trees shaking, liquefactions, dust clouds and jumping stones [Michetti et al. 2007].

The use of EEE for seismic intensity assessment has been recently promoted by the ESI 2007 scale, which evaluates earthquake size and epicenter solely from EEE. The application of ESI 2007 scale (i) allows the accurate assessment of intensity in sparsely populated areas, (ii) provides a reliable estimation of earthquake size with increasing accuracy towards the highest levels of the scale, where traditional scales saturate and ground effects are the only ones that permit a reliable estimation of earthquake size, and (iii) allows comparison among future, recent and historical earthquakes [Michetti et al. 2004]. In addition, some environmental morphogenetic effects (either primary or secondary) can be stored in the palaeoseismological record, allowing the expansion of the time window for seismic hazard assessment up to tens of thousands of years [Guerrieri et al. 2007, Porfido et al. 2007]. Furthermore, the EEE are not influenced by human parameters such as effects on people and the manmade environment as the traditional intensity scales (MCS, MM, EMS 1992, etc.) predominantly imply [Michetti et al. 2007].

The integration of the ESI 2007 intensity scale with the other scales including EMS-98, provides a better picture of the earthquake scenario, because only EEE allow suitable comparison of the earthquake intensity both (a) in time: effects on the natural environment are comparable for a time-window (recent, historic and palaeoseismic events) much larger than the period of instrumental record (last century), and (b) in different geographic areas: environmental effects do not depend on peculiar socio-economic conditions or different building practices.

Despite these advantages, there are some limitations in the use of the ESI 2007 scale. The ESI 2007 scale may not accurately describe the damage in the far field [Papanikolaou et al. 2009]. It is important to establish that this scale should be used predominantly in the epicentral area and thus may not accurately describe damage in the far field.

Also, in deep nonlinear morphogenic events [Caputo 2005], where ruptures cannot reach the surface, the ESI degrees should be correlated with the area, where severe EEE have been recorded. However, in such cases uncertainties are expected to be higher, implying that the assignment of the ESI 2007 intensities should probably be considered less precise for deep events [Papanikolaou et al. 2009].

Intensive EEE have not been expressed or even recorded in some earthquakes even though high grades were assigned using other macroseismic scales, due to the strictly localized area of damage and its limited geographical coverage. However, it is argued that this inconsistency is probably due to the structural response of multistorey buildings, the bedrock geology and the local site effects in accordance with the long distance from the epicenter.

This paper focuses on the June 8, 2008, Andravida earthquake (Mw=6.4) that affected the NW Peloponnese (western Greece) causing 2 fatalities and 214 injuries. The earthquake produced both extensive damage and significant EEE in the Ilia and the Achaia prefectures.

Five years after the event, we present some considerable data about the macroseismic characteristics of the earthquake and about the geology, tectonics and seismicity of the epicentral area (NW Peloponnese). This paper offers: (a) a view of the geotectonic and the seismotectonic regime of the region affected by the earthquake based on previous works and new field observations, (b) the description of the active faults and fault zones that pose seismic hazard for the residential parts of the region, (c) the evaluation of the seismic intensities based on the guidelines of the ESI 2007 scale [Michetti et al. 2007] and the EMS-98 scale [Grünthal 1998], (d) correlation of the seismic intensities with the geological, tectonic and geotechnical regime of the study area and (e) comparison of both seismic intensity scales and discussion on similarities and differences.

2. Geology

The geological formations in the study area can be divided into two major categories: alpine and post-alpine (Figure 1). The alpine formations belong to three major geotectonic units, the Pindos, Gavrovo and Ionian units [Philippson 1898, 1959, Renz 1955, Aubouin and Dercourt 1962, ESSO 1962, Christodoulou 1967, 1969, 1971, Tsoflias 1977, 1980, 1984, Dercourt et al. 1978, Fleury 1980, Fleury et al. 1981, Lekkas et al. 1992, 1995, Mariolakos et al. 1995], which outcrop towards the eastern sector of the study area (Figure 1). From the structural point of view, these geotectonic units form a succession of three nappes: the Pindos unit (first nappe) overthrusts the Gavrovo unit and the Gavrovo unit (second nappe) overthrusts the Ionian unit (third nappe) (Figure 1).

The Pindos unit crops out in the Panachaiko Mt and the Erymanthos Mts (Figure 1). The unit consists of clastic sediments of Upper Triassic, Lower Cretaceous and Tertiary age, Jurassic radiolarites and Upper Cretaceous pelagic limestones [Philippson 1898, 1959, Renz 1955, Fleury 1980, Tsoflias 1980, 1984, Dercourt et al. 1978, Fleury et al. 1981] (Figure 1).

The Gavrovo unit consists of the Upper Cretaceous-Upper Eocene shallow marine carbonates, which crop out on Skolis Mt and the thick Paleocene-Oligocene flysch, which crops out in the surrounding area [Fleury 1980, Tsoflias 1980, Fleury et al. 1981] (Figure 1).

The Ionian unit has a relatively poor exposure in the study area since it is unconformably overlain by post-alpine formations. It consists of the Jurassic-Eocene carbonate sequence [Aubouin and Dercourt 1962, Christodoulou 1967, 1969, 1971] and the Late Eocene-Early Oligocene overlying flysch exposed near Cape Araxos [Tsoflias 1977]. Moreover, the Triassic evaporates are observed in Kyllini peninsula [ESSO 1962, Christodoulou 1969, 1971, Tsoflias 1977, Lekkas et al. 1990, 1992, Mariolakos et al. 1995] (Figure 1).

The post-alpine formations occur in the northern, southern and western sector of the study area as parts of the Patras graben, the Kato Achaia-Fares and the Pyrgos-Olympia basins (Figure 1). They can be distinguished into Pliocene and Quaternary marine, lagoonal, lacustrine and terrestrial deposits and lie unconformably on the alpine basement [Christodoulou 1969, Tsoflias 1977, 1980, 1984, Kamberis et al. 1979, Fleury et al. 1981, Mariolakos et al. 1990, Lekkas et al. 1990, 1992, 2000, Mariolakos et al. 1995].

3. Neotectonics - Active tectonics

3.1. Introduction

NW Peloponnese is one of the most tectonically and seismically active regions of Greece [Mariolakos et al. 1995]. The intense tectonic activity from the Miocene to the Holocene resulted from its location on the external part of the present Hellenic orogenic arc and the close proximity to the present day NNW-SSE trending Hellenic subduction zone [Mariolakos et al. 1995] (Figure 1). Moreover, the diapiric phenomena of the Triassic evaporites originated between Tertiary and Quaternary and caused additional localized deformation [Hageman 1977, Winter 1979, Kowalczyk and Winter 1979, Underhill 1985, 1988, Mariolakos et al. 1990].

The neotectonic structure of the NW Peloponnese is characterized by the occurrence of large grabens or horsts bounded by E-W or NNW-SSE trending visible or concealed fault zones [Mariolakos et al. 1985] (Figure 1). Crucial role in the development of the post-alpine formations was played by the tectonic activity during the sedimentation phase, which created smaller horsts and grabens within the major neotectonic macrostructures [Lekkas et al. 2000]. Although these smaller structures are dynamically related, as they have resulted from an extensional stress field, which prevailed in the NW Peloponnese from the Early Pliocene up to present day [Doutsos et al. 1988, Lekkas et al. 1995, Koukouvelas et al. 1996, Doutsos and Kokkalas 2001, Papanikolaou et al. 2007], they followed different kinematic evolution [Mariolakos et al. 1995].

A great number of faults were active during Pliocene and Pleistocene, whereas others have also remained active during Holocene time [Lekkas et al. 1992, Fountoulis et al. 2013]. The recorded seismicity levels, which are among the highest in Greece [Hatzfeld et al. 1990], confirm the neotectonic studies, which show that the area is undergoing intense tectonic deformation. According to historical and instrumental records, numerous destructive earthquakes have taken place in the area since 399 BC [Galanopoulos 1955, 1981, Mariolakos et al. 1995, Papazachos and Papazachou 1997]. The major characteristics of the seismicity of the NW Peloponnese are that all major earthquakes occurred at shallow depths ($h < 20$ km) and had high intensities ranging from VI to IX [Galanopoulos 1955, 1981, Mariolakos et al. 1995, Papazachos and Papazachou 1997].

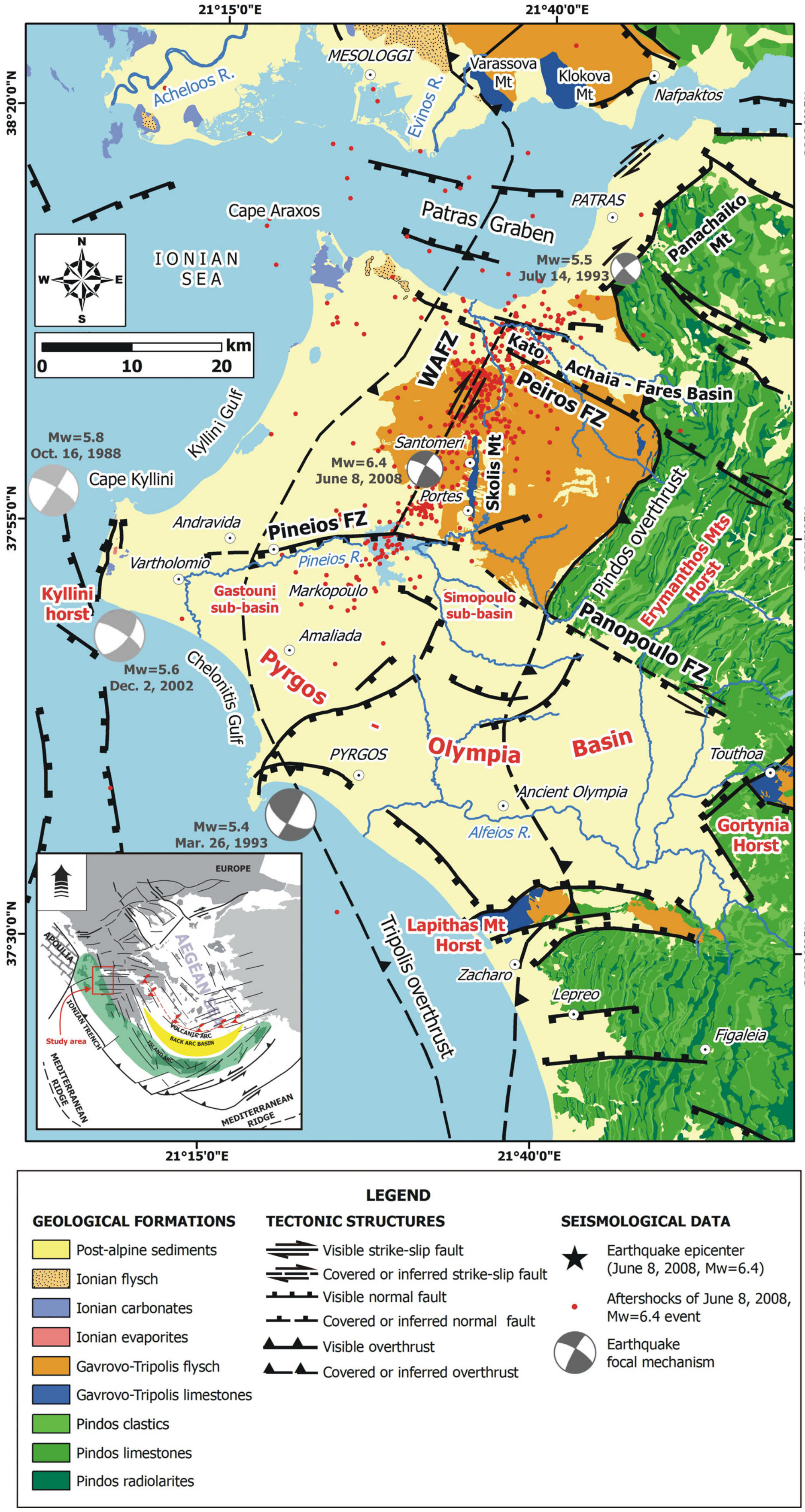

Figure 1. Geological map of the wider study area showing the major neotectonic macrostructures (Panachaiko Mt, Erymanthos Mts horst, Kato Achaia - Fares basin, Kyllini horst, Pyrgos - Olympia basin), the smaller neotectonic structures (Gastouni and Simopoulo sub-basins), the active fault zones based on Lekkas et al. [1992, 2000], Vassilakis et al. [2006], Mavroulis et al. [2010], Vassilakis et al. [2011] and Fountoulis et al. [2013] and the focal mechanisms of recent earthquakes in NW Peloponnese (1988 Kyllini, 1993 Patras, 1993 Pyrgos, 2002 Vartholomio, 2008 Andravida earthquakes) from Feng et al. [2010].

3.2. Neotectonic macrostructures of the study area

The structural damage and the EEE induced by the 2008 Andravida earthquake occurred in an area, where the following neotectonic macrostructures occur:

3.2.1. The Patras graben

The Gulf of Patras contains a WNW-ESE trending neotectonic graben structure [Ferentinos et al. 1985] (Figure 1), which is flanked to the NE by the mountains of Varassova and Klokova reaching an elevation of about 1000 m and composed of Cretaceous limestones and Eocene flysch of the Gavrovo unit [Richter and Mariolakos 1975, Mettos and Karfakis 1991, Papanikolaou and Lekkas 2008] (Figure 1). To the NW, it is fringed by Quaternary deltaic deposits of the Acheloos and the Evinos Rivers [Piper and Panagos 1981]. The southern shore is flanked by Pliocene-Quaternary deposits, which reach a maximum thickness of 1500 m [Hageman 1979]. Offshore drilling in the southern part of the graben reveals about 1800 m of Neogene and Pliocene-Quaternary sediments overlying Triassic anhydrites [Ferentinos et al. 1985].

Seismic profiling in the Gulf has shown that offshore Plio-Quaternary sediments are affected by widespread active faulting with a WNW-ESE trend [Ferentinos et al. 1985]. In the NE part of the Gulf, profiling records show that concealed faulting affects Pleistocene sequences beneath an undeformed Holocene surface layer. Onshore neotectonic data from around the Gulf show two groups of normal faults trending WNW-ESE and ENE-WSW [Ferentinos et al. 1985, Doutsos et al. 1987, 1988]. To the east of the Gulf, NNW-SSE and NNE-SSW normal faulting is observed [Kontopoulos and Doutsos 1985, Doutsos et al. 1987]. In addition, near-vertical faults have been observed in the same area that can be characterized as dip-slip or strike-slip faults (Figure 1).

3.2.2. The Pyrgos-Olympia basin

The Pyrgos-Olympia basin is a large graben bounded by the Erymanthos Mts horst towards N and NE, the Gortynia Mts (Tropaea) horst towards E and the Lapithas Mt horst towards S [Fountoulis and Lekkas 1991, Lekkas et al. 1992, 2000, Mariolakos et al. 1995, Fountoulis et al. 2007a,b] (Figure 1). These horsts consist of alpine formations and are bounded by fault zones forming impressive morphological discontinuities [Lekkas et al. 1992, 2000, Fountoulis et al. 2007a,b] (Figure 1). The basin is filled with Late Miocene-Holocene deposits, with a maximum thickness of approximately 3000 m [Lekkas et al. 2000]. These post-alpine deposits overlay unconformably the well-formed palaeorelief developed on the alpine formations [Lekkas et al. 2000].

The neotectonic evolution of the Pyrgos-Olympia basin was not the same in all its extent [Lekkas et al. 1992, 1994, Mariolakos et al. 1995]. It was influenced by the creation and evolution of smaller tectonic blocks (2nd order structures). Some of these 2nd order structures are affected by the presence of evaporites and the related diapiric phenomena (e.g. Kyllini horst) [Lekkas et al. 1992, Mariolakos et al. 1995].

3.2.3. The Erymanthos Mts horst

The Erymanthos mountain range is a NE-SW trending horst located E and SE of the Patras graben and NE of the Pyrgos-Olympia basin (Figure 1). It consists of alpine formations of the Pindos unit and specifically of the clastic sequence of Upper Triassic, Lower Cretaceous and Tertiary age, the Jurassic radiolarites and the Upper Cretaceous carbonate sequence [Tsoflias 1969, 1980, 1984, Dercourt et al. 1978, Fleury et al. 1981] (Figure 1). Fold axes and thrusts of the Pindos formations in the Erymanthos horst strike N 40-60° E and differ from the rest of the External Hellenides, where fold axes and thrusts strike N 10-30° W [Mariolakos et al. 1985, Mariolakos and Papanikolaou 1987]. The latter reflect the dextral rotation of Erymanthos Mts horst through the activation of E-W trending, sinistral strike slip faults [Mariolakos et al. 1985, Mariolakos and Papanikolaou 1987] (Figure 1).

3.3. Active fault zones

3.3.1. The Pineios fault zone

The Pineios fault zone is one of the youngest structures in NW Peloponnese [Mavroulis 2009, Mavroulis et al. 2010, Fountoulis et al. 2011a,b, 2013]. It is an approximately E-W trending active normal fault zone located SSW of Skolis Mt and dips southwards (Figure 1). The footwall consists of Upper Pliocene-Pleistocene formations uncomformably overlying the well-formed palaeorelief developed on the Gavrovo flysch, while the hanging wall consists of the aforementioned post-alpine formations and the Holocene alluvial deposits of the Lower Pineios River bed [Kamberis et al. 1979, Stamatopoulos et al. 1988, Fountoulis et al. 2013] (Figure 1).

3.3.2. The Panopoulo fault zone

The Panopoulo fault zone bounds the Erymanthos Mts horst in its southern part, trends NW-SE and dips to the SW. The footwall of the Panopoulo fault zone consists of alpine formations of the Gavrovo and the Pindos units [Dercourt et al. 1978, Fleury et al. 1981, Lekkas et al. 1992]. The hanging wall consists of Upper Pliocene-Pleistocene lacustrine or marine clays and Pleistocene terrigenous conglomerates of the Pyrgos-Olympia basin [Lekkas et al. 1992] (Figure 1).

The Panopoulo fault zone was formed between Mid-Upper Miocene and Upper Pliocene and it was active even during the Upper Pliocene-Pleistocene [Lekkas et al. 1992]. This fault zone is now entirely covered by recent formations and specifically by a soil horizon with thickness of several meters (5 m thick in the Panopoulo village area) [Lekkas et al. 1992].

3.3.3. The Peiros fault zone

South of the Patras Gulf, the Skolis Mt and the Araxos Cape consist of Mesozoic limestones (Figure 1). These outcrops suggest an intense tectonic uplift and erosion of the overlying thick Tertiary flysch. This uplift contrasts with the sea floor subsidence of the Patras Gulf and reveals the existence of a N-dipping normal fault in the southern part of the Gulf, parallel to the Kato Achaia coast [Dufaure 1975]. The western part of this fault occurs in the northern part of the study area and henceforth referred to as the Peiros fault zone (Figure 1). The Peiros fault zone trends NW-SE and dips towards NE. This fault zone propagates westwards to the Patras Gulf and it is reported as active due to: (a) the recorded deformation of the sea bed [Ferentinos et al. 1985], (b) the study of microseismicity [Melis et al. 1989] and (c) the high rates of Holocene subsidence [Chronis et al. 1991].

3.3.4. The western Achaia fault zone

The epicenter of the 2008 Andravida earthquake is located on a previously unknown almost vertical seismogenic zone, which is covered by Quaternary deposits and the thick Gavrovo flysch (Figure 1). Furthermore, there is no direct morphotectonic or geological evidence at surface [Mavroulis et al. 2010]. The fault plane solution of the earthquake is consistent with dextral strike-slip on a steep NE-SW trending fault (Figure 1). The distribution of the aftershock sequence also shows an alignment along a NE-SW trend for more than 60 km, revealing a structure sub-parallel to the dextral strike-slip Cephalonia transform fault zone [Konstantinou et al. 2009, Vassilakis et al. 2011]. We will refer to this NE-SW trending zone of deformation as the western Achaia fault zone (WAFZ).

4. The June 8, 2008, Andravida strike-slip earthquake (Mw=6.4)

On June 8, 2008, at 15:25 local time, an earthquake of Mw=6.4 struck the NW Peloponnese. It was the largest instrumentally recorded event in this area. It was felt throughout Peloponnese, western Greece and Attica, but predominantly in the Patras city and its suburbs. More than 15 villages and cities suffered significant damage. Three villages were evacuated in order to avoid rockfall risk during the aftershock activity. Overall, thousands of buildings suffered small to severe damage, whereas hundreds collapsed.

The epicenter was located in the Andravida area, 35 km SW from the city of Patras (Figure 1). The main shock is consistently located at depths 19-24 km if different absolute locations are considered and at 18 km depth after wave cross correlation (WCC) relocation method [Konstantinou et al. 2009]. All provided focal mechanisms demonstrate a NE-SW trending strike-slip seismic fault zone that dips towards NW at a steep angle (Figure 1). The spatial distribution of aftershock seismicity with most hypocentral depths in the range between 15 and 25 km [Konstantinou et al. 2009] was clearly aligned along a NE-SW axis for a total length of about 60 km (Figure 1). This is consistent with the strike of one of the two nodal planes indicated by the focal mechanism of the main shock.

The Andravida earthquake is the largest but not the first strike-slip event in the recent history of the NW Peloponnese. Strike-slip earthquakes are common in western Greece and are due to a compressional component of the differential motion between the Africa and Eurasian plates [Benetatos et al. 2004]. Over 30 additional dominantly strike-slip crustal earthquakes with Mw>4.0 have been recorded between 1965 and 2009 in the NW Peloponnese and the surrounding regions from published reports and earthquake catalogues. Apart from the microseismic experiments carried out by Hatzfeld et al. [1989, 1990], recent studies of seismicity in Peloponnese recorded earthquakes with focal mechanisms, that indicate dextral strike-slip motion in the NW Peloponnese [Hatzfeld et al. 2000, Sachpazi et al. 2000, Benetatos et al. 2004]. Recent strike-slip events in this area include the offshore Kyllini earthquake in October 16, 1988 (Mw=5.8), and the offshore Vartholomio earthquake in December 2, 2002 (Mw=5.6) [Lekkas et al. 1990, 1995, Mariolakos et al. 1991, 1995, Roumelioti et al. 2004] (Figure 1). These events were generated about 30-40 km WSW of the 2008 Andravida event.

A broad and multidisciplinary effort was conducted by several research groups in campaigns of instrumental measures and surveys [Ganas et al. 2009, Konstantinou et al. 2009, Feng et al. 2010, Papadopoulos et al. 2010]. Special attention was also devoted to the description and mapping of the effects induced by the Andravida earthquake on the natural and the manmade environment. Numerous groups of scientists have contributed to the collection of these data [Lekkas et al. 2008a,b, Margaris et al. 2010, Pavlides et al. 2008, Ganas et al. 2009, Konstantinou et al. 2009, Koukouvelas et al. 2010, Mavroulis et al. 2010, Feng et al. 2010, Papadopoulos et al. 2010], which are presented below in detail.

5. Andravida earthquake environmental effects (EEE)

Several EEE have been recorded and presented in Table 1 and Figures 2 and 3.

5.1. Primary EEE

No effects, which are directly linked to the earthquake energy and in particular to the surface expression of the seismogenic source, were induced by the 2008 Andravida strike-slip earthquake. There was no primary surface faulting observed and the surface deformation was smaller compared to the Andravida earthquake magnitude. The burial depth and downdip extent of the seismogenic fault within a homogeneous elastic earth cannot explain the observed small surface deformation. Therefore, Feng et al. [2010] argue that the compositionally weak, 3 km thick flysch layer acted as a near-surface decoupling agent, which isolates subsurface deformation from the surface. Particularly, the strain energy released by the thick pile of flysch probably could not sustain the coseismic rupture propagation below the pre-orogenic carbonates to the surface; alternatively the weak flysch may allow for an essentially decoupled cap with lower overall stress, and hence lateral slip in the carbonates will not necessarily propagate through the flysch layer [Feng et al. 2010]. The remaining strain in the flysch during coseismic rupture might be released by interseismic ductile deformation or fail in subsequent, smaller earthquakes [Feng et al. 2010].

5.2. Secondary EEE

5.2.1. Surface fractures

Surface fractures were among the most characteristic secondary effects triggered by the 2008 Andravida earthquake implying a $\mathrm{VIII}_{\mathrm{ESI\text{-}2007}}$ intensity (Table 1, Figures 2, 3). They were observed (a) in the Kato Achaia area, (b) in the Nissi area and (c) in the Dafni area (Table 1, Figures 2, 3). The Kato Achaia town and the Dafni village are located at the northern and the southern ends of the aftershocks distribution respectively, while the Nissi village is located west of the surface projection of the seismogenic dextral strike-slip fault zone (Figure 2).

Surface fractures in the Kato Achaia area occurred in Holocene loose formations and especially in coastal and alluvial deposits (Table 1, Figure 2). The coastal deposits consist of fine and coarse grained materials (sands, pebbles) with poor coherence. Their thickness is small ranging from 1 m to several meters and the width of the outcrops varies. Their geomechanical behavior and properties vary widely depending on their particle size distribution and their mineralogical composition, while small scale subsidence and swelling phenomena are frequently observed. The alluvial deposits are loose, include clays, silts, sands and pebbles and are easily erodible and leached by surface water. Their frequent and rapid changes in their lithological composition and grain size distribution vertically and horizontally control their physical and mechanical properties, while their thickness, their lithological anisotropy and the morphological slope affect their behavior especially in the case of dynamic loading.

The NE-SW trending surface fractures observed in Kato Achaia show a dominant strike-slip component. These fractures exceed 300 m in length and 5 cm in width with a horizontal displacement estimated to be around 20 cm. Some NW-SE trending extensional fractures were also observed in the area. Despite the fact that the fractures in the Kato Achaia area have the same NE-SW trend with the seismogenic strike-slip WAFZ that caused the Andravida earthquake, they could not be considered as primary effects and as the surface expression of the WAFZ due to their limited length and width. An intensity $\mathrm{VIII}_{\mathrm{ESI\text{-}2007}}$ was assigned for the Kato Achaia surface fractures (Table 1, Figure 4).

NW-SE trending transverse surface fractures were observed in the Nissi area, in Holocene loose torrential deposits consisting of clayey-sandy materials with gravels and cobbles (Table 1, Figures 2, 3a,b). They present similar characteristics and behavior to those of the alluvial deposits mentioned above. They were 300 m long, 20 cm wide, at least 1.5 m deep and their vertical throw was estimated to be around 40 cm, with uplift on the western side. The horizontal displacement of approximately 20 cm shows significant strike-slip component. An intensity $\mathrm{VIII}_{\mathrm{ESI\text{-}2007}}$ was assigned for the Nissi surface fractures (Table 1, Figure 4).

Transverse extensional surface fractures trending NW-SE were also observed in the Dafni area on a Pleistocene marine formation with medium to coarse-grained sands and well-bedded grits with intercalations of medium-grained sandstones (Table 1, Figures 2, 3c). It is characterized by medium to high coherence and low resistance in weathering. An intensive fracturing is usually present, while the manifestation of shallow rotational and/or translational slides is frequently observed. Its mechanical characteristics and behavior are strongly influenced by the degree of saturation, so that in case of full saturation a considerable reduction of shear strength is observed. These surface fractures

Sites (in Figure 2)	Coordinates		Type of EEE	Description of EEE	ESI 2007 Intensity - Effects in the environment
	Longitude	Latitude			
Kato Achaia area	21.333680114	38.083577846	Secondary effect, Surface fractures	NE-SW trending surface fractures with a dominant strike-slip component Length: 300 m Width: 5 cm Horizontal displacement: 20 cm	VIII - Heavily damaging / Extensive
	21.334612499	38.083207950			
	21.340100602	38.085919865			
Kato Achaia area (sea shore of the Kato Achaia town)	21.334215760	38.085654912	Secondary effect, Liquefaction	(a) Ejected grey sandy material forming vent fractures with length ranging from 50 cm to 4 meters and width up to 22 cm (b) Sand volcanoes with diameter up to 8 cm in an area of 1 km^2, accompanied by two ground cracks with horizontal displacement of 4 cm toward the sea and vertical subsidence of 2 cm	VIII - Heavily damaging / Extensive
Kato Achaia area (Alikes)	21.313602890	38.084280626	Secondary effect, Liquefaction	(a) sand volcanoes with diameter ranging from 4 to 12 cm (b) ejection of sandy material from small cracks on the pavement (c) lateral spreading	VII - Damaging / Appreciable
Kato Achaia area	21.325247331	38.075948882	Secondary effect, Liquefaction	Ejection of grey sands	VI - Slightly damaging / Modest
Kato Achaia area	21.364415315	38.075855135	Secondary effect, Slope movements	Landslide (volume < 10 m3)	V - Strong / Marginal
	21.353815502	38.080655047	Secondary effect, Slope movements	Landslide (volume < 10 m3)	V - Strong / Marginal
Nissi village	21.235887630	38.005173843	Secondary effect, Surface fractures	NW-SE trending (transverse) surface fractures Length: 300 m Width: 20 cm Depth: 1.5 m Vertical throw: 40 cm Horizontal displacement: 20 cm	VIII - Heavily damaging / Extensive

Table 1. List of sites with the EEE triggered by the June 8, 2008, Andravida earthquake (Mw=6.4).

Sites (in Figure 2)	Coordinates		Type of EEE	Description of EEE	ESI 2007 Intensity - Effects in the environment
	Longitude	Latitude			
Nissi	21.232432301	38.001358310	Secondary effect, Liquefaction	Small sand volcano	VI - Slightly damaging / Modest
Dafni area	21.284705860 21.283409919 21.283355847	37.562397350 37.563521140 37.562108882	Secondary effect, Surface fractures	NW-SE trending (transverse) extensional surface fractures Length: hundreds of meters Width: 10 cm Depth: 1.5 m	VIII - Heavily damaging / Extensive
Close to the Roupakia village (shore of the Pineios artificial lake)	21.302713420	37.525539307	Secondary effect, Liquefaction	(a) 2 sand-mud boils with diameter up to 85 cm and 3 smaller ones with diameter up to 70 cm each (b) Vent fractures with length more than 5 meters and width up to 15 cm (c) Sand volcanoes with diameter up to 17 cm (d) Lateral spreading at the Pineios River banks	VIII - Heavily damaging / Extensive
Close to the Kalivakia village (shore of the Pineios artificial lake)	21.310759358	37.534371297	Secondary effect, Liquefaction	Ejection of fine-grained material from ground fissures	VI - Slightly damaging / Modest
Oinoi area (Pineios River banks)	21.313918848	37.500249714	Secondary effect, Liquefaction	(a) Ejection of coarse-grained material from small ground cracks (b) Horizontal displacement of 1-2 cm towards the river	VI - Slightly damaging / Modest
Manolada beach	21.193831519	38.031359923	Secondary effect, Liquefaction	Small sand boils involving clear sand	VI - Slightly damaging / Modest
Kounoupeli	21.205468581	38.055762768	Secondary effect, Hydrological anomalies	(a) Renewed flow of the curative springs of Yrmini in Kounoupeli area (b) Smaller surficial flows along the same coast (c) Turbidity of water in several wells and springs	VI - Slightly damaging / Modest
Tsoukaleika	21.382714877	38.084855302	Secondary effect, Slope movements	Landslide (volume <10 m^3)	V - Strong / Marginal

Table 1 (continued from previous page). List of sites with the EEE triggered by the June 8, 2008, Andravida earthquake (Mw=6.4).

Sites (in Figure 2)	Coordinates		Type of EEE	Description of EEE	ESI 2007 Intensity - Effects in the environment
	Longitude	Latitude			
Vrachneika	21.395829218	38.092803508	Secondary effect, Slope movements	Sliding of marls along bedding planes and joints dipping towards the road (volume <10 m^3)	V - Strong / Marginal
Portes (western steep slopes of the Skolis Mt)	21.343057309	37.560517620	Secondary effect, Slope movements	Rock toppling failures of limestones (volume <10 m^3)	V - Strong / Marginal
Santomeri (western steep slopes of the Skolis Mt)	21.343339906	37.590362705	Secondary effect, Slope movements	Rock toppling failures of limestones at the western slopes of the Skolis Mt (volume <10 m^3)	V - Strong / Marginal
Road from Portes to Valmi	21.324217909	37.540554416	Secondary effect, Slope movements	Sliding of formations consisting of alternations of marly clays, silts, sands with consolidated or non-consolidated conglomerates (volume <10 m^3)	V - Strong / Marginal
Pigadi and Simiza area	21.233510597	37.542134671	Secondary effect, Slope movements	Landslides along the active Pineios fault zone (volume <10 m^3)	V - Strong / Marginal
Porto Katsiki	20.325317214	38.352500073	Secondary effect, Slope movements	Landslide (volume <10 m^3)	V - Strong / Marginal
Diakofto	22.115590708	38.111568534	Secondary effect, Slope movements	Sliding of marls along bedding planes and joints dipping towards the road (volume <10 m^3)	V - Strong / Marginal
Lefkochori	22.005041384	37.404163374	Secondary effect, Slope movements	Rock toppling failures of limestones along the active Lefkochori fault zone (volume <10 m^3)	V - Strong / Marginal
Latzoi	21.332694557	37.422065603	Secondary effect, Slope movements	Landslide (volume <10 m^3)	V - Strong / Marginal
Neraida	21.394094201	37.434676681	Secondary effect, Slope movements	Landslide (volume <10 m^3)	V - Strong / Marginal

Table 1 (continued from previous two pages). List of sites with the EEE triggered by the June 8, 2008, Andravida earthquake (Mw=6.4).

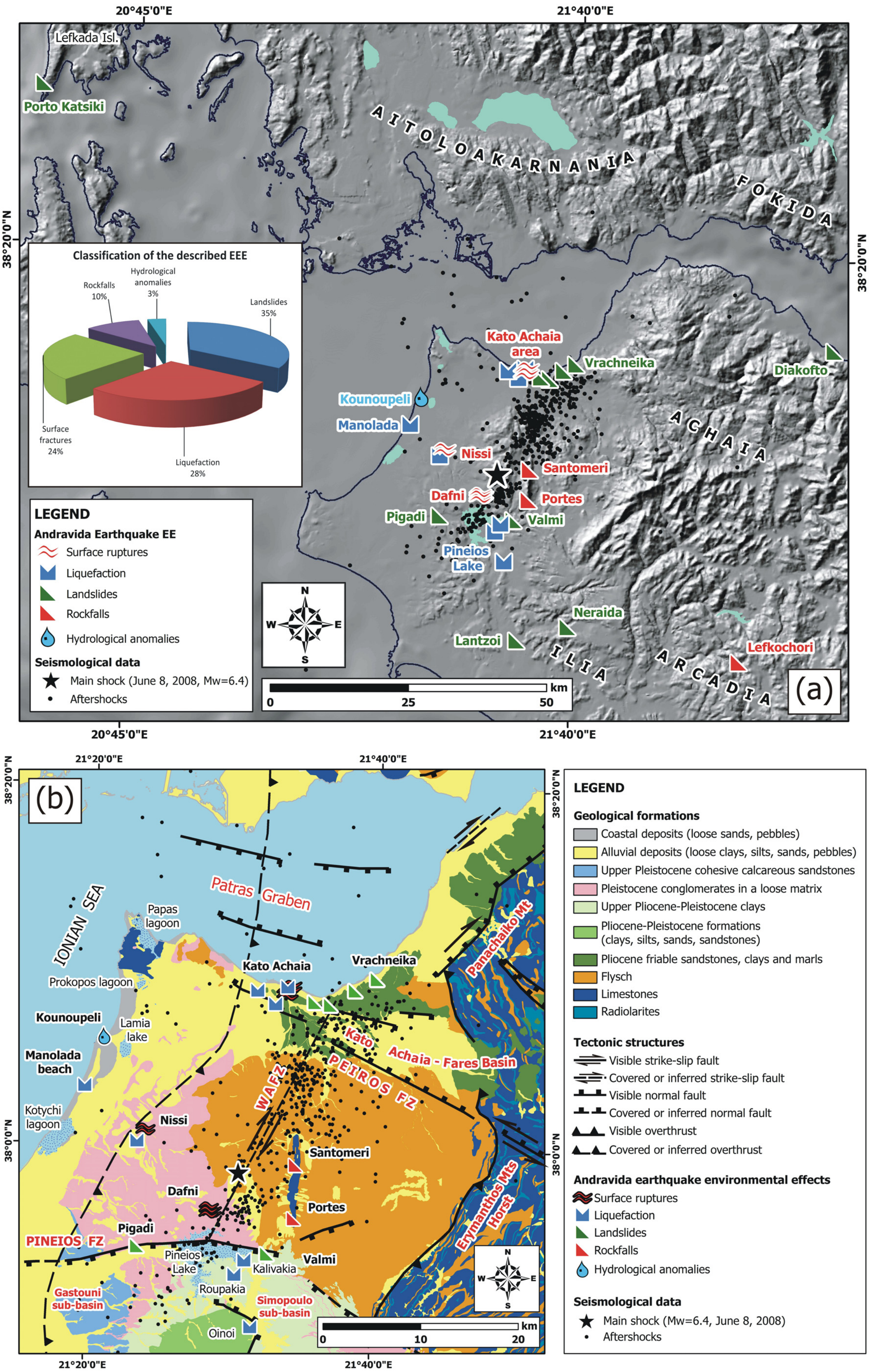

Figure 2. The spatial distribution of the 2008 Andravida EEE in (a) the NW Peloponnese wide area and (b) in the epicentral area of the 2008 Andravida earthquake according to the Table 1. The percentage distribution of the Andravida EEE by type is also presented. The epicenter distribution for the Andravida aftershock sequence is from the aftershocks catalogue presented by the Department of Seismotectonics, Earthquake Planning and Protection Organization (from June 8 to June 20, 2008) [Lalechos et al. 2008].

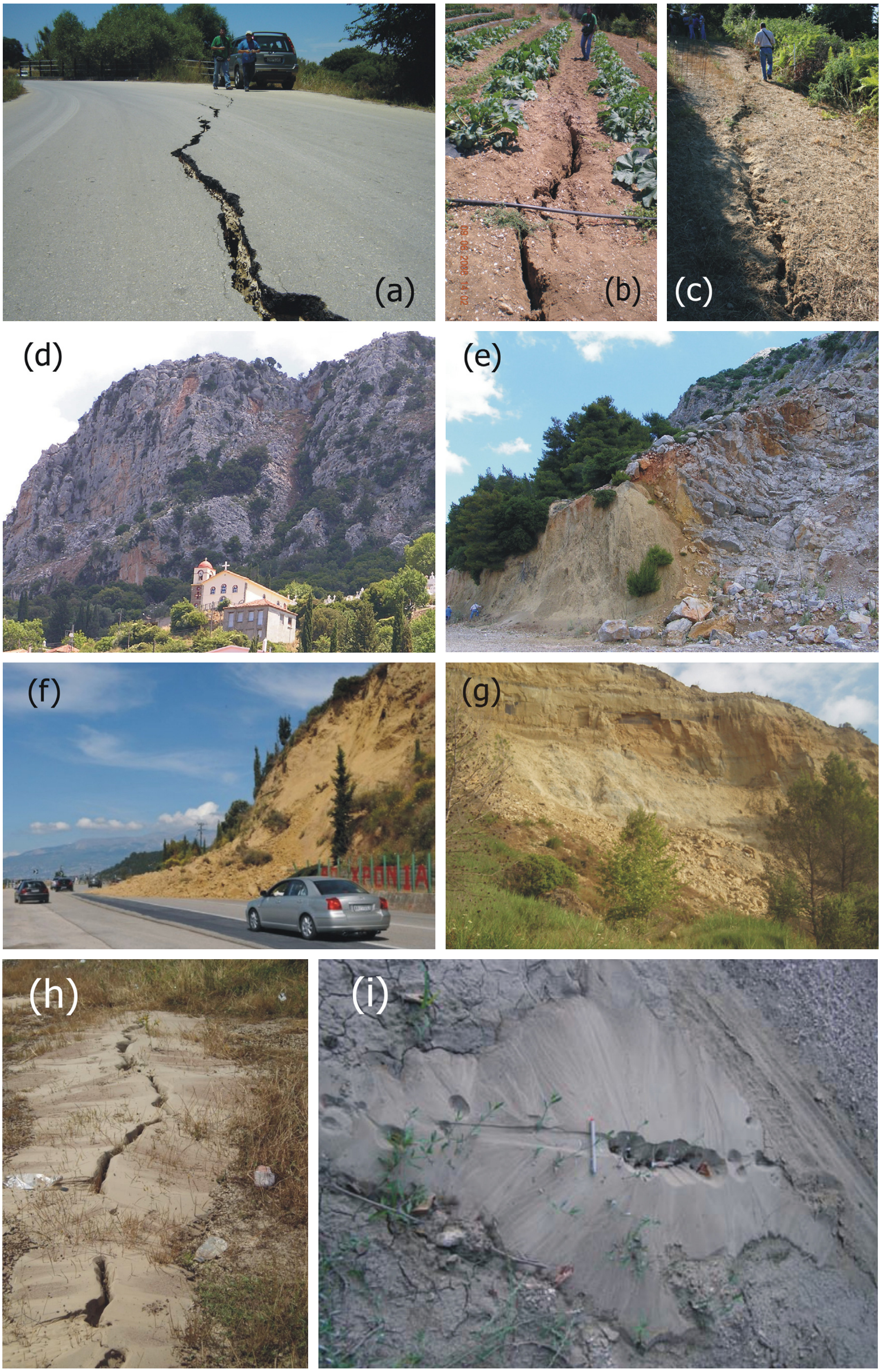

Figure 3. View of the most characteristic 2008 Andravida EEE. (a, b, c) NW-SE trending transverse surface fractures were observed in the Nissi area. (d, e) Rock toppling failures of limestones took place at the western foothills of Skolis Mt, in the Santomeri (d) and the Portes (e) villages. (e) Cretaceous carbonates overthrust shaly flysch at the western steep slopes of Skolis Mt. The flysch strata close to the thrust surface are steeply dipping and overturned. (f) Landslides and failures of artificial slopes took place along the national roads of the study area (Vrachneika). (g) Landslide along the road from the Portes to the Valmi village. (h) Surface fractures and flows of liquefied material observed in the Kato Achaia area. (i) Sand boils in the Nissi area.

were 10 cm wide and at least 1.5 m deep. An intensity $VIII_{ESI-2007}$ was assigned for the Dafni surface fractures (Table 1, Figure 4).

5.2.2. Liquefaction phenomena

Impressive liquefaction phenomena were concentrated in sites formed by loose alluvial deposits, both at the areas located north (Kato Achaia, Alikes and Nissi) and south (Roupakia, Kalivakia, Oinoi) of the epicenter [Papathanassiou et al. 2008] (Table 1, Figures 2, 3). It is important to note that no liquefaction phenomena were observed in the Lower Pineios River delta area, where liquefaction and other forms of ground failure were observed during the previous offshore earthquakes of October 16, 1988, in Kyllini peninsula presented and described by Mariolakos et al. [1989, 1995] and Lekkas et al. [1990] and of December 2, 2002, in Vartholomio presented and described by Apostolidis et al. [2002].

Typical examples of liquefaction phenomena were reported at the Pineios River Lake (Figure 2). This area consists of loose mainly fine-grained alluvial deposits of the Pineios River (Figure 2b), which present poor coherence, small scale subsidence and swelling phenomena. At the shore of the Pineios artificial lake, close to the Roupakia village (Figure 2b), the following liquefaction phenomena were reported: (a) two sand-mud boils with diameter up to 85 cm and three smaller ones with diameter up to 70 cm each, (b) vent fractures with length more than 5 meters and width up to 15 cm, (c) sand volcanoes with diameter up to 17 cm and (d) a lateral spreading at the Pineios River banks [Papathanassiou et al. 2008] (Table 1). Therefore, the assigned intensity for this area is $VIII_{ESI-2007}$ (Table 1, Figure 4).

Fine-grained material was ejected from ground fissures at the Pineios River shore close to the Kalivakia village (Figure 2b), while coarse-grained material was ejected from small ground cracks at the Pineios River banks, few kilometers to the south [Papathanassiou et al. 2008] (Table 1). At the same place, a horizontal displacement of 1-2 cm towards the river was observed. The assigned intensity for both areas is $VI_{ESI\ 2007}$ (Table 1, Figure 4).

Impressive liquefaction phenomena were also observed in the loose coastal and alluvial deposits of the Kato Achaia area (Figure 2) including: (a) ejected grey sandy material forming vent fractures with length ranging from 50 cm to 4 m and width up to 22 cm and (b) sand volcanoes with diameter up to 8 cm in an area of 1 km^2, accompanied by two ground cracks with horizontal displacement of 4 cm toward the sea and vertical subsidence of 2 cm [Papathanassiou et al. 2008] (Table 1). Hence, intensity $VIII_{ESI-2007}$ was assigned (Table 1, Figure 4).

Close to a stream estuary located 2 km west of the Kato Achaia town (Alikes area), liquefaction phenomena were also observed including: (a) sand volcanoes with diameter ranging from 4 to 12 cm, (b) ejection of sandy material from small cracks on the pavement and (c) lateral spreading (Table 1). An intensity $VII_{ESI-2007}$ was assigned for the Alikes site (Table 1, Figure 4).

A small sand volcano was also observed in loose alluvial deposits in the Nissi village (Figure 2b). Minor liquefaction phenomena also occurred at the Manolada beach (Figure 2b) and they were manifested as small sand boils involving clear sand. An intensity $VI_{ESI-2007}$ was assigned for both sites (Table 1, Figure 4).

5.2.3. Slope movements

The 2008 Andravida earthquake triggered a number of small (volume $< 10\ m^3$) and isolated slope movements in several localities over a wide area including the NW Peloponnese, Aitoloakarnania and Ionian Islands (Table 1, Figures 2, 3). These slope movements include: (a) sliding of marls along bedding planes and joints dipping towards the national road from Patras to Pyrgos near Vrachneika ($V_{ESI\ 2007}$) and towards the national road from Patras to Corinth near Diakofto ($V_{ESI\ 2007}$), (b) rock toppling failures of limestones in the eastern margin of the Pyrgos-Olympia basin, along the Lefkochori fault zone, which is active [Fountoulis et al. 2007a,b] ($V_{ESI\ 2007}$), (c) landslides along the active Pineios fault zone in the wider area of Pigadi and Simiza villages ($V_{ESI\ 2007}$), (d) rock toppling failures of limestones in the wider area of Santomeri and Portes villages at the western slopes of the Skolis Mt ($V_{ESI\ 2007}$), (e) sliding of formations consisting of alternations of clays, silts, sands with consolidated or non-consolidated conglomerates along the road from Portes to Valmi village ($V_{ESI\ 2007}$) and along the road near Tsoukaleika village in the Achaia prefecture and near Latzoi and Neraida in the Ilia prefecture. Other slope movements and particularly rockfalls were also observed northwestwards as far as the Porto Katsiki beach in the island of Lefkada ($V_{ESI\ 2007}$) (Table 1, Figures 2, 3).

In the evaluation of the total area of the distribution of the EEE and the ESI 2007 intensities, it is recommended not to include isolated effects which occurred in the far field. Therefore, the slope movements observed in the SW part of the Lefkada Isl. (Porto Katsiki), in the eastern part of the Achaia prefecture (Diakofto village), in the central-western Peloponnese (Lefkochori village) and in the Pyrgos municipality (Latzoi and Neraida villages) (Figure 2a) were not taken into account for the final assignment of the environmental seismic intensities of the study area.

Landslides in the Kato Achaia, Vrachneika and Tsoukaleika areas occurred in friable Pliocene sandstones, sandy clays and clayey marls with sparse intercalations of conglomerates (Figures 2b, 3f). The lithological facies of this formation are variable. The non-uniform and anisotropic behavior of the formation as a whole and the rapid change of its mechanical characteristics vertically and horizontally resulting from its heterogeneity cause the generation of shallow failures and slides along natural and artificial slopes, as happened in the areas above.

Landslides in the area of the Pigadi and the Simiza villages occurred in a Pleistocene marine formation with medium to coarse-grained sands and well-bedded grits with intercalations of medium-grained sandstones. This formation is faulted by the active Pineios fault zone [Fountoulis et al. 2013] (Figures 1, 3b). The tectonic deformation along this active fault zone resulted in a dense net of discontinuities and the relatively loose formations facilitated these slope movements.

Landslides along the road from the Portes to the Valmi village were observed in an Upper Pliocene-Lower Pleistocene formation consisting of clays, silts, sands with conglomerates, with varying coherence, strong heterogeneity and high anisotropy in its behavior.

Skolis Mt is the most impressive topographic feature of the study area, a N-S trending steep mountain, reaching an altitude of 1000 m, rising above the lower flysch relief. Cretaceous carbonates overthrust shaly flysch at its western flank [Fleury 1980, Tsoflias 1980, Fleury et al. 1981]. The flysch strata close to the thrust surface are steeply dipping and overturned (Figure 3e) clearly revealing the intense tectonic deformation of the area. The Gavrovo Cretaceous carbonates are also highly fractured by E-W trending inactive faults [Lekkas et al. 1992]. This intense and multiple fracturing along with the erosion and weathering processes contribute to the decreased cohesion along the steep slopes of the mountain and resulted in the generation of rockfalls during the 2008 Andravida event (Figures 2b, 3d,e).

Rockfalls also occurred in the eastern margin of the Pyrgos-Olympia basin (Figure 2a) and are linked to the highly fractured carbonates of Tripolis unit along the Lefkochori fault zone, which is active [Fountoulis et al. 2007a,b]. This is an area where suitable conditions for the generation of rockfalls already existed before the earthquake, which simply triggered these phenomena.

Rockfalls in the NW part of the Lefkada Isl. (Figure 2a) are directly linked to the active faults defining the neotectonic unit of Lefkata peninsula [Lekkas et al. 2001] and forming the impressive fault scarps in Cretaceous limestones of the Paxoi unit [Lekkas et al. 2001] observed along the Porto Katsiki beach.

5.2.4. Hydrological anomalies

Hydrological phenomena were observed in hot springs and wells including renewed flow of springs and changes in water discharges as well as water turbidity. The renewed flow of the curative springs of Yrmini in Kounoupeli area was reported by Pavlides et al. [2008] (Table 1, Figure 2). These coastal springs located northwest of Nea Manolada and the hot water spring from NW-SE trending cracks occurred in limestones of the Ionian unit as well as from an IGME drilling. It is remarkable that the flow had been stopped since the offshore 1988 Kyllini earthquake and reestablished after the 2008 Andravida earthquake with larger discharge rates. Artesian phenomena and out-flows causing damage of the borehole sealing have also been identified. Considering the aforementioned data, an intensity $VI_{ESI\text{-}2007}$ was assigned for the site of Kounoupeli.

Smaller surficial flows were detected along the same coast in a NW-SE direction. Moreover, water turbidity was reported in several wells and springs in the flat area between Nea Manolada and Vartholomio villages.

5.3. Conclusions on the EEE and the corresponding ESI 2007 intensities

In total, secondary effects in 29 sites have been recorded, described, mapped and classified in the following four categories: seismic fractures (24%), liquefaction phenomena (28%), slope movements (45%) [including landslides (35%) and rockfalls (10%)], and hydrological anomalies (3%) (Table 1, Figures 2, 3). The total areal distribution of secondary EEE is about 800 km^2. Based on this total area, the ESI 2007 epicentral intensity degree is VIII-IX and closer to IX (Figure 4).

The Andravida EEE are classified as marginal to extensive. A maximum $VIII_{ESI\ 2007}$ intensity has been assigned to several sites (Kato Achaia, Nissi and Pineios Lake areas) (Table 1, Figures 2, 4), where surface fractures up to 20 cm wide and up to hundreds meters long as well as impressive liquefaction phenomena were observed in post-alpine formations. Intensity $VII_{ESI\ 2007}$ was assigned to the Dafni area, where surface fractures were observed. A minimum intensity equal to V was observed within the alpine basement (western slopes of Skolis Mt) as well as in the post-alpine formations (Pigadi, Simiza, Valmi and Vrachneika villages) respectively, where small volume (<10 m^3) rockfalls and landslides were triggered. An ESI 2007 intensity map was constructed depicting the spatial distribution of the effects and the isoseismals based on the ESI 2007 intensities (Figure 4).

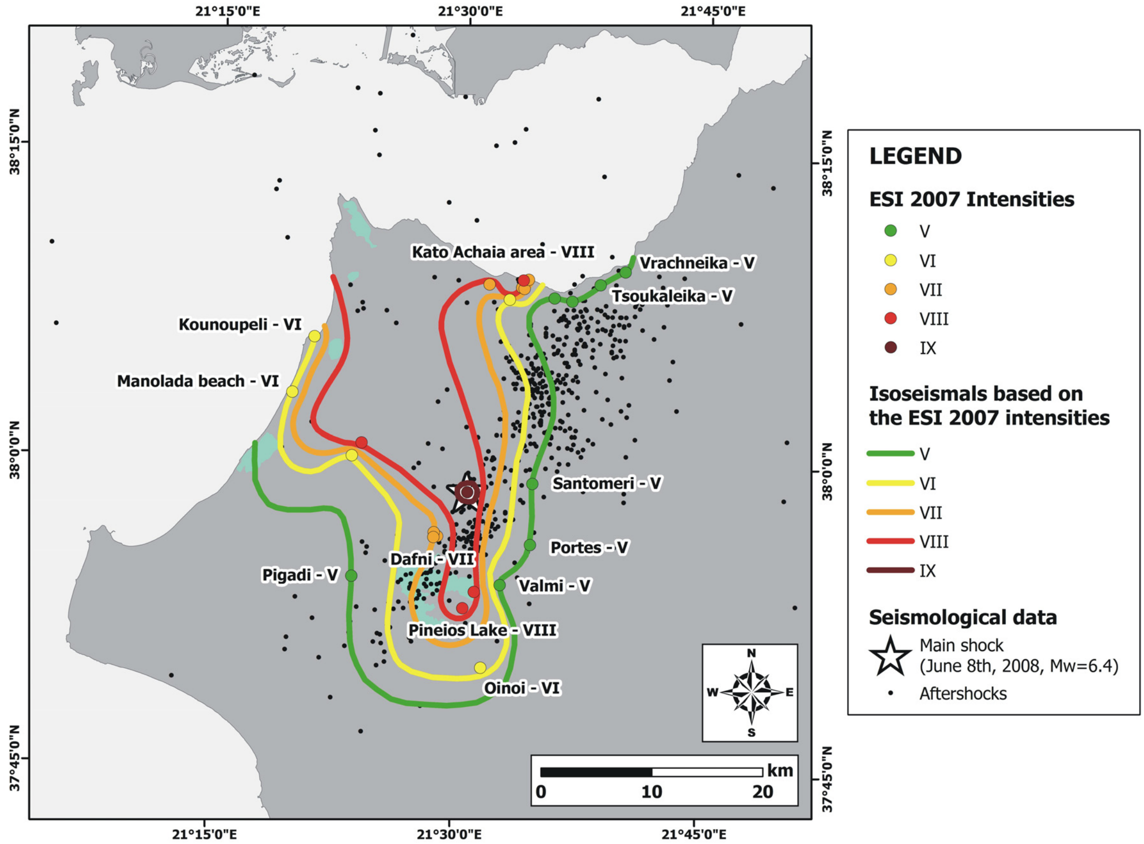

Figure 4. The 2008 Andravida earthquake isoseismal map based on the ESI 2007 intensities.

6. Structural damage in the affected area and EMS-98 intensities

6.1. Type of structures and structural damage

The majority of structures in the study area can be broadly categorized in two main types, which are: (a) one or two storey stone masonry buildings with insufficient or non-existent seismic resistance design and (b) reinforced concrete (R/C) buildings. Most of the R/C buildings were built according to the Greek Seismic Code that was implemented in 1959 with subsequent revisions and upgrades.

After detailed engineering surveys and evaluations of the earthquake affected buildings in western Greece (conducted by the Earthquake Recover Service of the Greek Ministry of Infrastructure, Transport and Networks), 1874 buildings were considered unsafe to occupy (580, 1266 and 28 red carded buildings in Ilia, Achaia and Aitoloakarnania prefectures respectively), while 5630 buildings were considered suitable only for restricted use or access until repairs are completed (2330, 2902 and 398 yellow carded buildings in Ilia, Achaia and Aitoloakarnania prefectures respectively) (http://www.yas.gr).

Structural damage to masonry buildings induced by the 2008 Andravida earthquake includes (a) substantial to heavy damage (grade 3) comprising large and extensive cracks in most walls and fall of very large pieces of plaster (Figure 5a), (b) very heavy damage (grade 4) including partial collapse of walls (Figure 5b) and (c) destruction (grade 5) comprising total or near total collapse of the building (Figure 5c). Damage in most of the R/C buildings was concentrated in non-load carrying components, infill and partition walls, comprising (a) moderate damage (grade 2) such as diagonal cracking in brick partition walls as an influence of prevailing shear forces in brick partition walls and panels (Figure 5d), (b) substantial to heavy damage (grade 3) including detachments of the walls from the surrounding R/C frame (Figure 5e) and (c) destruction of the R/C building (grade 5) comprising collapse of ground floor due to damage to R/C elements (Figure 5f).

Extensive damage was observed to the highly vulnerable monumental buildings and especially to churches and their bell towers including (a) cracks observed at the exterior walls as well at the junctions of the exterior walls, at several interior masonry arches and around openings or at the top of the exterior walls on which wood roofs rest (Figure 5g), (b) partial collapse of the exterior walls (Figure 5h) and (c) total collapse of the building (Figure 5i).

Damage to bridges included cracks in the road asphalt surface, transverse to the longitudinal axis of the bridge (Figure 5j,k,l).

Bending of railway lines with 20 cm displacement due to seismic fractures has been observed in the Kato Achaia railway station (Figure 5m).

Figure 5. Structural damage induced by the 2008 Andravida earthquake: (a) damage of grade 3 to masonry building in the Nissi village including large and extensive cracks in most walls and fall of very large pieces of plaster, (b) damage of grade 4 to masonry building in the Valmi village including partial collapse of walls, (c) damage of grade 5 to masonry building in the Valmi village including total or near total collapse, (d) damage of grade 2 to R/C building in the Stafidokampos village including diagonal cracking in brick partition wall, (e) damage of grade 3 to R/C building in the Valmi village including detachments of the walls from the surrounding R/C frame and (f) damage of grade 5 to R/C building in the Didacheika village including collapse of ground floor due to damage to R/C elements, (g, h, i) damage to monumental buildings including (g) cracks observed at the exterior walls as well at the junctions of the exterior walls, at several interior masonry arches and around openings or at the top of the exterior walls on which wood roofs rest (Nissi village), (h) partial collapse of the exterior walls (Psari area), (i) total collapse of the church (Valmi village). (j, k, l) Damage to bridges included cracks in the road asphalt surface, transverse to the longitudinal axis of the bridge (Kato Achaia area). (m) Railway line in the Kato Achaia train station deformed by the earthquake.

6.2. EMS-98 intensities

Based on field surveys immediately after the main shock aiming at the description, mapping and classification of the damage induced by the earthquake on infrastructure and constructions in the NW Peloponnese [Lekkas et al. 2008a,b,c, Margaris et al. 2008, 2010, Mavroulis 2009, Mavroulis et al. 2010, Papadopoulos et al. 2010], EMS-98 intensities were assigned to the localities that suffered damage by the earthquake. An isoseismal map was also constructed and depicts the spatial distribution of the structural damage and the isoseismals based on the EMS-98 intensities (Figure 6).

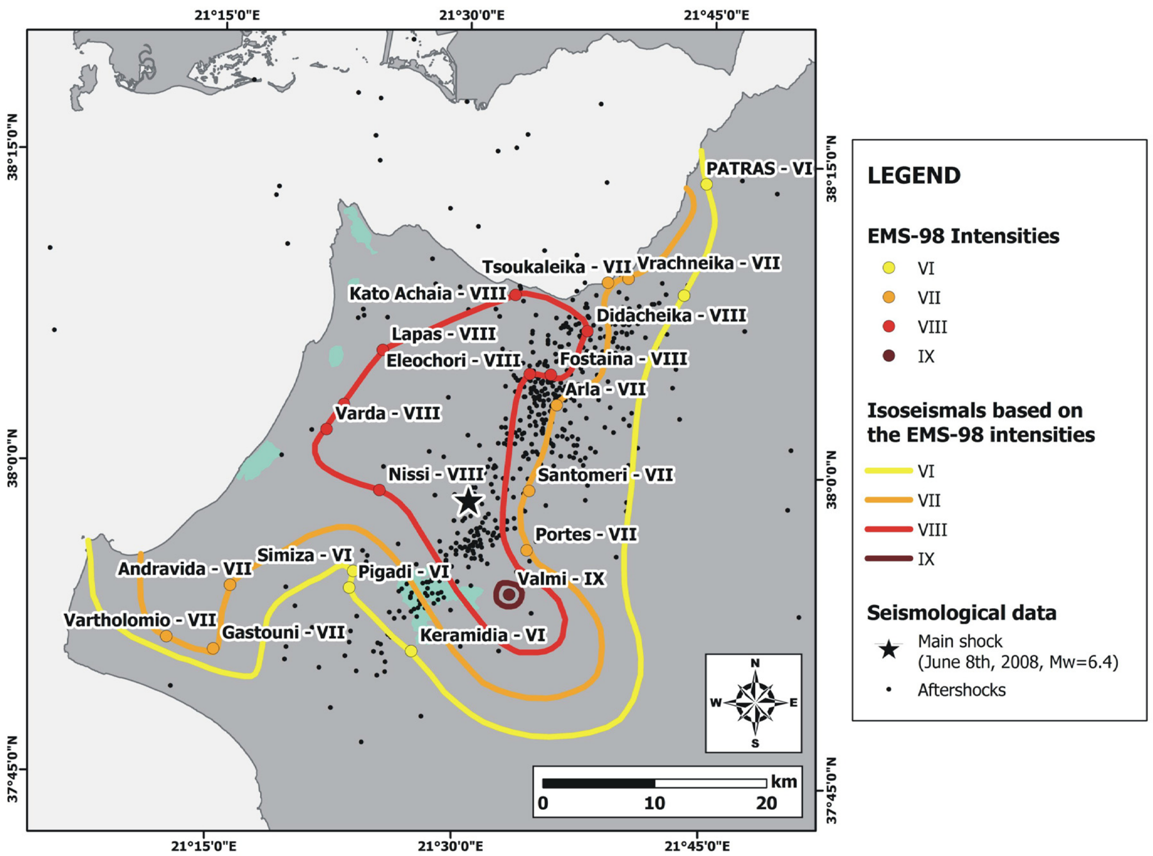

Figure 6. The 2008 Andravida earthquake isoseismal map based on the EMS-98 intensities.

Damage due to shocks between building of different height and stiffness or observations from special structures, such as lighthouses, radio towers, bridges etc. were not taken into account for the EMS-98 seismic intensity assignments for the 2008 Andravida event always bearing in mind the limitations and the special cases of the EMS-98 scale. The damage to monumental buildings, such as churches and their bell towers are only presented below and have been not taken into account for the EMS-98 seismic intensity assignments.

The maximum EMS-98 intensity was assigned to the Valmi village (IX_{EMS-98}) (Table 2, Figure 6) located close to the eastern tip of the active Pineios fault zone and founded on an Upper Pliocene-Pleistocene formation consisting of sandy or silty clays with local intercalations of coarse-grained sands with varying coherence, strong heterogeneity and high anisotropy in its behavior. It is estimated that 85% of the masonry buildings in the Valmi village were considered unsafe to occupy suffering damage ranging from grade 3 (large and extensive cracks in most walls and fall of very large pieces of plaster) to grade 5 (total or near total collapse) (Figure 5b,c). Many (40-50%) R/C buildings suffered moderate damage of grade 2, as cracking of load-carrying components were observed especially in columns and joists (Figure 5e) and a few (5%) of grade 3, as brick infill walls were detached from the surrounding R/C frame.

Kato Achaia is the area that was shaken most vio-

Town/Village	EMS-98	ESI 2007
Valmi	IX	V
Kato Achaia	VIII	VIII
Didacheika	VIII	
Fostaina	VIII	
Eleochori	VIII	
Nissi	VIII	VIII
Varda	VIII	
Nea Manolada	VIII	
Lapas	VIII	
Santomeri	VII	V
Portes	VII	V
Vartholomio	VII	
Gastouni	VII	
Andravida	VII	
Vrachneika	VII	V
Tsoukaleika	VI	V
Pigadi	VI	V
Simiza	VI	V

Table 2. EMS-98 and ESI 2007 intensities obtained in the region.

lently and sustained much damage to its buildings in the northern part of the affected area. It is located close to the northern tip of the activated blind strike slip fault zone and founded on the Peiros River alluvial deposits, which are characterized by frequent and rapid changes in their lithological composition and grain size distribution vertically and horizontally. Many (40 %) masonry buildings suffered damage of grade 4, as they sustained serious failure of walls and partial structural failure of roofs and floors and a few of them had to be demolished. A few (10 %) masonry buildings underwent damage of grade 5, as they totally or almost totally collapsed. A few (5 %) R/C buildings suffered damage of grade 2, as cracks were observed in the brick infill walls. The estimated EMS-98 intensity in these villages was as high as VIII (Table 2, Figure 6).

Many churches both in the Valmi village (Figure 5i) and the Kato Achaia town collapsed or underwent serious structural damage. Extensive cracking was observed at the exterior walls as well as in almost every interior arch and dome that constitute its structural system. Damage to several masonry bell towers were also observed in many cases due to the different height and stiffness between the main church building and the masonry bell towers.

The Didacheika, the Fostaina and the Eleochori villages are located within the Kato Achaia-Fares basin. The first is founded on old Quaternary deposits consisting of polygenic, loose conglomeratic breccia with terra rossa and local intercalations of red clayey sand, while the other two villages are founded on the Gavrovo flysch sediments consisting mainly of pelites and conglomerates. These three villages suffered similar damage to those of Kato Achaia. Thus, the estimated EMS-98 intensity in these villages was as high as VIII (Figure 6). Many (30-40%) one-storey and two-storey masonry buildings underwent damage of grade 5, as they were totally or partially collapsed and another 10% suffered severe structural damage in the Fostaina village. A few (5%) of the R/C buildings of the Didacheika village experienced cracking of the brick fill walls and detachments of the walls from the surrounding R/C frame, while one collapsed possibly due to constructional defect.

In the above mentioned areas of Didacheika, Fostaina and Elaiochori, it seems that the foundation factor (subsurface composed mainly of old Quaternary deposits and flysch sediments) was the predominant cause of damage. The surficial flysch beds usually show a medium to strong weathering and a dense net of discontinuities causing secondary looseness. This formation gives a weathering mantle of varying thickness. Its geotechnical behavior is anisotropic and controlled by the degree of looseness, the orientation of discontinuities, the dip of slopes and the action of water. The behavior of the old Quaternary deposits is controlled by the thickness, their lithological anisotropy and the slope angle, especially in the case of dynamic loading. Furthermore, the dominant cause for the damage in many structures as well as for the inconsistency between the higher EMS-98 compared to the ESI 2007 values in several villages was the poor building quality. Buildings are highly vulnerable since they are predominantly old masonry buildings with no earthquake-resistant design.

The Nissi village is located northwest of the earthquake epicenter and founded on loose Pleistocene torrential deposits consisting of sands in the lower beds and rubbles in the upper beds as well as on a Pleistocene formation of medium to coarse-grained sands and well-bedded grits with medium coherence, low resistance in weathering and intensive fracturing. The most widely observed damages in masonry buildings of the Nissi village were the cracking of the load-carrying walls and the detachment of large pieces of plasters applied on walls (grade 3), serious failure of load-carrying walls (grade 4) and the total or almost total collapse of the construction (grade 5). A $\mathrm{VIII}_{\mathrm{EMS\text{-}98}}$ intensity was assigned (Table 2, Figure 6).

The villages of Varda, Nea Manolada and Lapas are located north of the Nissi area. They are founded on Pleistocene formations and alluvial deposits consisting mainly of clayey-sandy material and gravels. The structural damage and the EMS-98 intensity (VIII) are similar to those of the Nissi village.

Structural damage also occurred in the western slopes of the Skolis Mt especially in the Santomeri and Portes villages (Figures 1, 3). Rockfalls from the steep slopes of Skolis Mt consisting of Gavrovo limestone over-thrusting flysch caused damage of grade 5 to one of the masonry buildings in the Santomeri village. Many (50%) masonry buildings suffered damage of grade 3, as large and extensive cracking and failure of partition and brick infill walls were observed and a few (10%) of them sustained damage of grade 4, as they underwent serious failure of walls. Similar damage and percentage of the damaged buildings were reported in the neighboring Portes village. Thus, a $\mathrm{VII}_{\mathrm{EMS\text{-}98}}$ intensity was assigned in the Santomeri and Portes villages (Table 2, Figure 6).

Another area that suffered structural damage is the Pyrgos-Olympia basin with Gastouni and Simopoulo sub-basins (Figure 1), which are filled with loose Holocene deposits, Upper Pleistocene coherent calcareous sandstones, Pleistocene conglomerates in a loose siliceous matrix and Pliocene-Pleistocene clays, silts, sands and sandstones [Kamberis 1987, Lekkas et al. 1992] (Figure 1). The thickness, the strong heterogeneity, the lithological anisotropy of these formations results in the non-uniform and the high anisotropic behavior of the formations and the rapid change of the mechanical characteristics in the different horizons both vertically and laterally. Damage of grade 1 was observed in a few (5%) of the R/C buildings including cracking of brick infill walls and hairline cracks of columns as an extension of cracks in non-load carrying components. The usual damage of grade 3 in many (30%) masonry buildings and damage of grade 4 in a few (10%) of them were also observed. A $VII_{EMS\text{-}98}$ intensity was assigned in this area (Table 2, Figure 6).

In Vrachneika and Tsoukaleika founded on coastal and alluvial deposits, few masonry buildings (20 %) suffered negligible to slight damage. A few (5 %) of the R/C buildings suffered slight damage such as fine cracks in plaster and fall of small pieces of plaster. A $VI_{EMS\text{-}98}$ intensity was assigned in the Vrachneika and Tsoukaleika villages (Table 2, Figure 6).

7. Discussion

The identification of the previously unknown dextral strike-slip fault zone that generated the 2008 Andravida earthquake provides useful information regarding the internal deformation of the area. It is evident that a lot of settlements located in the NW Peloponnese are exposed to significant seismic hazard due to the proximity to several active fault zones and faults (e.g. Pineios, Panopoulo, Peiros, WA fault zones) capable of storing enough potential energy to rupture and generating major devastating earthquakes.

The analysis of the field observations allowed us to map the spatial distribution of EEE and structural damage and assign seismic intensities based on the ESI 2007 and EMS-98 scales. The assigned seismic intensities allowed us to construct the respective isoseismal maps for the Andravida earthquake. This information is essential for the identification and characterization of the most vulnerable sites exposed to the occurrence of earthquake environmental effects (seismically induced liquefaction phenomena, slope movements, ground settlements, etc.), the better assessment of the future impact of a similar event on towns and villages like these in the NW Peloponnese that are characterized by strong urban and infrastructural growth.

The evaluated ESI 2007 intensities were compared with the assessed intensities based on the EMS-98 scale (Table 2, Figure 7). The maximum ESI 2007 intensity based on the parameters and the total area of the distribution of the secondary EEE is VIII-IX, while the maximum EMS-98 intensity is IX. The $VIII_{ESI\ 2007}$ is mostly observed NW of the surface projection of the seismogenic strike-slip WAFZ, while the $IX_{EMS\text{-}98}$ is observed E of this fault zone. For all the sites where intensity VIII has been recorded the ESI 2007 and the EMS-98 agree, but for others the ESI 2007 intensities values are lower by one or two degrees than the corresponding EMS-98 ones, as it is clearly concluded from the comparison of the produced isoseismals (Table 2, Figure 7). An exception to this rule is the Valmi village, where considerable structural damage occurs along with the lack of significant EEE, so that the $V_{ESI\ 2007}$ intensity is four degrees lower than the $IX_{EMS\text{-}98}$ intensity (Table 2, Figure 7).

Firstly, we have to consider that the ESI 2007 intensity scale is calibrated on the basis of only seismically induced ground effects and does not take into consideration the earthquake effects on structures and the perceptibility of the strong ground motion. Therefore, where no or limited ground damage is observed, for instance in the almost total destroyed Valmi village, where no coseismic primary and insignificant secondary environmental effects were observed, the ESI 2007 scale provide seismic intensity lower than the traditional macroseismic intensity scales, underestimating the overall effects of an earthquake to the manmade environment.

Moreover, the generation of several earthquakes that struck the NW Peloponnese in recent years including Kyllini (October 16, 1988, Mw=5.8), Pyrgos (March 3, 1993, Mw=5.4), Patras (July 14, 1993, Mw=5.4) and Vartholomio (December 2, 2002, Mw=5.6) earthquakes (Figure 1), had certainly weakened the stone masonry buildings, many of them constructed using fluvial stones and poor quality mortar, which had been badly or inadequately restored afterwards. Thus, in the rural area of the NW Peloponnese, which is mostly constructed according to the first Greek Seismic Code or with insufficient or nonexistent seismic resistance design, the evaluation of the intensity based only on the EMS-98 scale may overestimate the "strength" of the earthquake and the ground shaking. The opposite is likely in urban areas constructed according to modern code provisions, where the evaluation of the seismic intensity based only on EMS-98 scale may underestimate the "strength" of the earthquake and the ground shaking.

Guerrieri et al. [2009] have drawn similar conclusions after the application of the ESI 2007 scale and the MCS scale for the 1997 Umbria-Marche (Central Italy) seismic sequence and the comparison of the corresponding intensities. The ESI 2007 intensity values have frequently resulted one degree or even more lower than the MCS ones, with some exceptions. This variability between the ESI 2007 and the MCS intensity values is predominantly attributed to the poor maintenance of buildings due to the inconstant habitation. So, the MCS

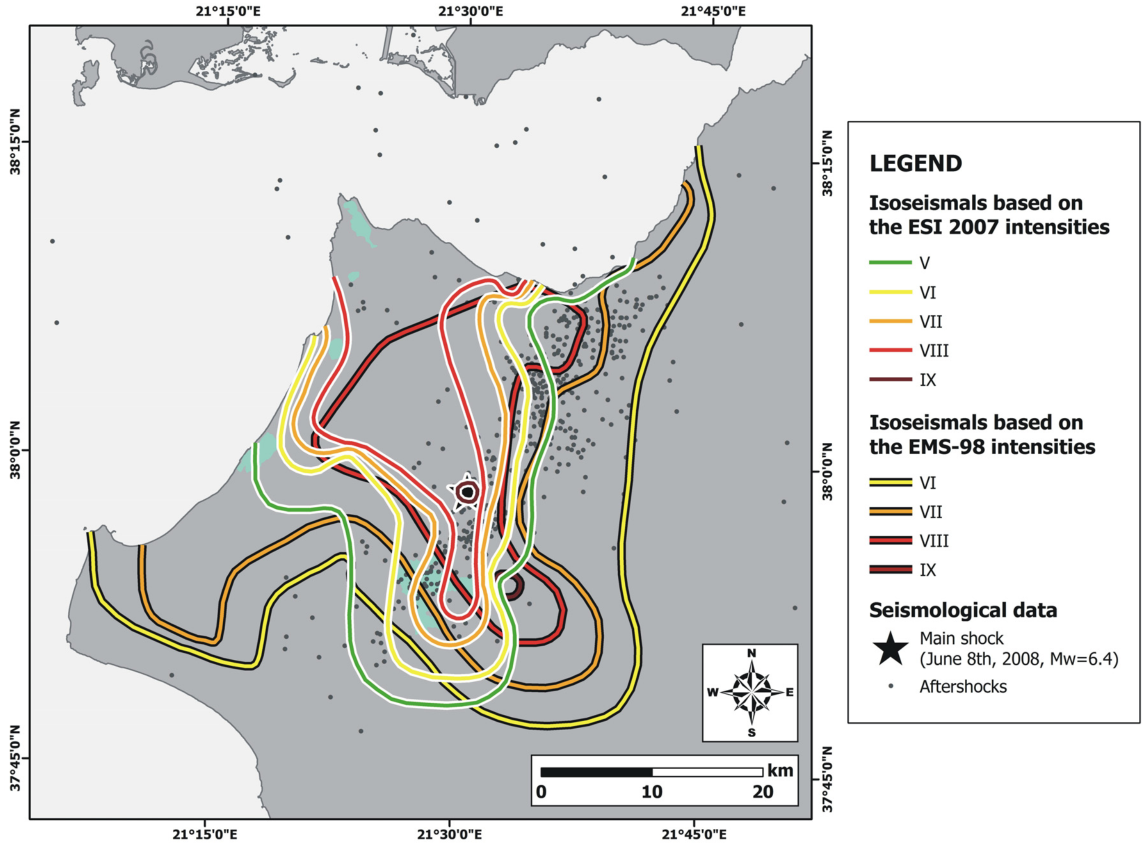

Figure 7. Comparison, similarities and differences between ESI 2007 and EMS-98 intensities and isoseismals for the 2008 Andravida earthquake.

intensity field has resulted slightly overestimated with respect to what expected for an event of Mw=5.6 in the Apennines.

Therefore, it is concluded that the integration of the ESI 2007 scale with the EMS-98 scale and other traditional intensity scales provides a better picture of the earthquake effect on the built and the natural environment. The combined evaluation of the constructed isoseismal maps based on the ESI 2007 and EMS-98 seismic intensities have once more confirmed the crucial role of the EEE and the structural damage in the process of seismic intensity assignments and the seismic hazard assessment in the NW Peloponnese. They can be also evaluated and used in mitigation strategies, community preparedness and response planning as well as in disaster management in the case of a future event of similar or larger magnitude.

Furthermore, the application of the recently introduced ESI 2007 scale for the 2008 Andravida strike-slip event enlarges the dataset from earthquakes from different tectonic settings and especially from moderate strike-slip events. The fact, that this moderate strike-slip event did not trigger primary but only secondary environmental effects, can also be used to infer the threshold magnitude for surface faulting in the NW Peloponnese and to calibrate palaeoearthquake size from both primary and secondary effects.

The recent introduction of the ESI 2007 scale, due to its quantitative nature, also promises to offer higher objectivity in the process of assessing macroseismic intensities particularly in the epicentral area than do traditional intensity scales that are influenced by human parameters. The ESI 2007 scale follows the same criteria (EEE) for all events and can compare not only events from different tectonic settings, but also contemporary and future earthquakes with historical events. It offers higher spatial resolution and coverage and incorporates also site effects. As a result, a re-appraisal of historical and recent earthquakes so as to constrain the ESI 2007 scale may prove beneficial for the seismic hazard assessment by reducing the uncertainty implied in the attenuation laws and eventually in the seismic hazard maps [Papanikolaou 2011]. As more data from earthquakes from different tectonic settings as well as recent and past historical events are gathered enlarging the dataset and requiring no need for intensity scale conversions, the compilation of an ESI 2007 intensity attenuation relationship should be one of the future goals for seismic hazard assessment [Papanikolaou 2011]. The ESI 2007 will definitely make an impact in seismic hazard assessment in the near future if, as expected, could reduce this uncertainty.

8. Conclusions

No primary EEE were induced by the 2008 Andravida earthquake. However, secondary EEE were widely observed including seismic fractures, liquefaction phenomena, slope movements (rockfalls and landslides) and hydrological phenomena in hot springs and wells. The majority of sites in the NW Peloponnese are characterized by ESI 2007 intensities lower by one or two degrees than the corresponding EMS-98 ones.

The spatial distribution of the Andravida earthquake aftershocks indicates a linear NE-SW trending seismogenic structure. This is consistent with the strike of one of the two nodal planes indicated by the focal mechanism of the main shock revealing a NE-SW dextral strike-slip fault zone. No significant surface fractures of this orientation were observed during our field reconnaissance of the NW Peloponnese. The only closely spaced set of fractures that are in agreement with this direction is the one observed in the Kato Achaia area. However, they cannot be considered as primary effects that are directly linked to the earthquake energy and in particular to the surface expression of the seismogenic structure due to their limited length and width. The other observed directions of surface fractures are characterized as secondary effects induced by the ground shaking and were caused by the differential seismic response of several loose lithologies, the lateral instability of surficial formations (e.g. fractures in the Nissi area) and the liquefaction of the underlying formations (e.g. fractures in the Kato Achaia area). The various trends are due to the geometry of slopes (e.g. fractures in the Dafni area), the orientation of bedding planes of fine- and coarse-grained phases, the presence of morphological discontinuities and the instability conditions in the vicinity of drainage channels (e.g. fractures in the Nissi and Dafni areas), canals and coastlines (e.g. fractures in the Kato Achaia area).

Slope movements were associated with the strong ground shaking. They were due to: (a) the presence of geological formations with mechanical characteristics that make formations susceptible to failure, (b) the strong heterogeneity and the rapid change of the mechanical characteristics in the different horizons both vertically and horizontally resulting in non-uniform and anisotropic mechanical behavior of formations, (c) the intense and multiple fracturing, erosion and weathering contributing to the decreased cohesion along the western steep slopes of the Skolis Mt as well as (d) the intense tectonic deformation along active fault zones resulting in a dense net of discontinuities and sectors of decreased cohesion and formations loosening.

Liquefaction phenomena were observed close to river banks and coastlines (e.g. the Pineios and Peiros Rivers banks, stream bank in the Nissi area, the Kato Achaia and Manolada coastal areas). They occurred due to the local soil conditions, the shallow water table and the earthquake loading.

The EEE induced by the 2008 Andravida earthquake were generally not aligned in specific orientations, but concentrated in the northern and southern tip of the WAFZ as well as close to and northwest of the epicenter of the main shock. This distribution of EEE includes the surface projection of the causative dextral strike-slip WAFZ, but the area, where maximum seismic intensities ($VIII_{ESI\ 2007}$) occur, is observed north and northwest of the causative WAFZ and is not identical with the surface projection of the zone.

Generally, surface faulting associated to strike-slip events of Mw=6.4 is about 13 km in length and 30 cm in max displacement according to the equations presented by Wells and Coppersmith [1994]. Thus, the lack of surface faulting and the observed small surface deformation induced by the 2008 Andravida earthquake is smaller compared to its magnitude and not characteristic for a Mw=6.4 strike-slip event with this focal depth. The burial depth and downdip extent of the fault within a homogeneous elastic earth cannot explain the observed small surface deformation. Therefore, Feng et al. [2010] argue that the compositionally weak, 3 km thick flysch layer acted as a near-surface decoupling agent, which isolates subsurface deformation from the surface. Particularly, the strain energy released by the thick pile of flysch probably could not sustain the coseismic rupture propagation below the pre-orogenic carbonates to the surface. Alternatively, the weak flysch may allow for an essentially decoupled cap with lower overall stress, and hence lateral slip in the carbonates will not necessarily propagate through the flysch layer [Feng et al. 2010]. The remaining strain in the flysch during coseismic rupture might be released by interseismic ductile deformation or fail in subsequent, smaller earthquakes [Feng et al. 2010].

According to the EMS-98 classification of buildings damage [Grünthal 1998], damage to masonry buildings ranged from grade 3 to grade 5, while damage in most of R/C buildings ranged from grade 1 to grade 3. Monumental buildings and special structures also suffered extensive damage. It is concluded that the severity and the distribution of the structural damage is controlled by the following factors:

(a) The local geological and soil conditions. The western flat area as well as the central and the southern hilly area, where the most extensive damage occurred, consist mainly of Neogene and Quaternary deposits. It is important to note that the earthquake damage was comparatively smaller in villages founded on the alpine basement (e.g. intensity $VII_{EMS\text{-}98}$ was assigned to Portes and Santomeri villages on the western slopes of Skolis Mt).

The Neogene deposits are mainly fine-grained and the Quaternary deposits are (i) loose and mainly coarse-grained or mixed coarse- and fine-grained phases and (ii) coherent and mainly coarse-grained or mixed coarse-and fine-grained phases. They are particularly sensitive to dynamic loading and they are easily erodible and leached by surface water. They are characterized by intense heterogeneity of their mechanical characteristics in different horizons both vertically and horizontally resulting in anisotropic mechanical behavior. The manifestation of rotational and/or translational slides is frequent. Differential settlements usually take place in areas with a predominance of clays and clayey marls.

Moreover, the central area consists of flysch that usually show a medium to strong weathering and a dense net of discontinuities, causing intense secondary looseness. Landslide phenomena occurred with an increased frequency, usually affecting weathering mantle and upper fragmentation zone. The geotechnical behavior presents a clear anisotropy and rapid changes controlled by the orientation of discontinuities, the dip of slope, the action of surface water and the degree of looseness.

(b) The construction type of buildings. The Andravida earthquake caused moderate to very heavy structural damage (grade 3-5) to masonry buildings including houses with one or two stores and insufficient or nonexistent seismic resistance design. Most of the R/C buildings constructed according to the revised and upgraded Greek Seismic Code sustained damage ranging from nil to moderate (grades 1-3) having an adequate response during this earthquake.

Acknowledgements. Professor Ioannis Fountoulis sadly passed away (16/2/2013) before the publication of this article. He was a dear friend and colleague who left too soon. He will be an inspiration to us, never forgotten and immeasurably missed. Dr. Christoph Grützner and an anonymous reviewer are acknowledged for the constructive comments and helpful suggestions that improved the paper. Dr. Raúl Pérez-López is also acknowledged for the careful editing assistance.

References

Apostolidis, E., D. Galanakis and H. George (2002). Report of macroseismic observations in the Vartholomio region (Ilia prefecture) after the earthquake of 02/12/2002, IGME, Athens, Unpublished Report, 41 pp. (in Greek).

Aubouin, J., and J. Dercourt (1962). Zone préapulienne, zone ionienne et zone du Gavrovo en Péloponnèse occidental, Bulletin de la Société Géologique de France, 4, 785-794.

Benetatos, C., A. Kiratzi, C. Papazachos and G. Karakaisis (2004). Focal mechanisms of shallow and intermediate depth earthquakes along the Hellenic Arc, Journal of Geodynamics, 37, 253-296.

Caputo, R. (2005). Ground effects of large morphogenic earthquakes, Journal of Geodynamics, 40 (2-3), 113-118.

Castilla, R.A., and F. Audemard (2007). Sand blows as a potential tool for magnitude estimation of pre-instrumental earthquakes. Journal of Seismology, 11, 473-487.

Christodoulou, G. (1967). About the age of Kastro limestones, NW Peloponnese, Greece, Greek Geological Society Publication, 7, 121-136 (in Greek).

Christodoulou, G. (1969). Geological Map of Greece: Vartholomio sheet, scale 1:50,000, IGME 1969, Athens.

Christodoulou, G. (1971). Über die Neogene Ablagerunen im Gebiet von Kyllini (NW Peloponnes), IGME, Special Publication, 11, 1-60.

Chronis, G., D.J.W Piper and C. Anagnostou (1991). Late Quaternary evolution of the Gulf of Patras, Greece: Tectonism, deltaic sedimentation and sea-level change, Marine Geology, 97, 191-209.

Dengler, L., and R. McPherson (1993). The 17 August 1991 Honeydaw earthquake north coast California: a case for revising the Modified Mercalli Scale in sparsely populated areas, Bulletin of the Seismological Society of America, 83, 1081-1094.

Dercourt, J., F. Meilliez, J.M. Flament and P. De Wever (1978). Geological Map of Greece: Kertezi sheet, scale 1: 50,000, IGME 1978, Athens.

Doutsos, T., N. Kontopoulos and D. Frydas (1987). Neotectonic evolution of northwestern-continental Greece, Geologische Rundschau, 76, 433-452.

Doutsos, T., N. Kontopoulos and G. Poulimenos (1988). The Corinth-Patras rift as the initial stage of continental fragmentation behind an active island arc (Greece), Basin Research, 1, 177-190.

Doutsos, T., and S. Kokkalas (2001). Stress and deformation patterns in the Aegean region, J. Struct. Geol., 23, 455-472.

Dowrick, D.J. (1996). The Modified Mercalli earthquake intensity scale - Revisions arising from recent studies of New Zealand earthquakes, Bulletin of the New Zealand Society for Earthquake Engineering, 29 (2), 92-106.

Dufaure, J.J. (1975). Le relief du Péloponnèse, Thèse d'état Univ. Paris IV, France, 1422 pp.

Earthquake Recover Service of the Greek Ministry of Infrastructure, Transport and Networks, http://www.yas.gr.

Esposito, E., S. Porfido, G. Mastrolorenzo, A.A. Nikonov and L. Serva (1997). Brief review and preliminary proposal for the use of ground effects in the macroseismic intensity assessment, In: Ye Hong (ed.), Proceedings 30th International Geological Congress

(Beijing, China, August 4-14, 1996), VSP, Utrecht, The Netherlands, 5, 233-243.

ESSO (L. Perry and G.P. Temple) (1962). Unpublished geological reports about the Paxoi, Zakynthos-Kyllini, Filiatra and Pylos oil concession areas.

Feng, L., A.V. Newman, G.T. Farmer, P. Psimoulis and S. Stiros (2010). MW 6.4 Achaia-Elia Earthquake in northwestern Peloponnese, Greece: an indicator of an immature transform fault zone, Geophys. J. Int., 183, 103-110.

Ferentinos, G., M. Brooks and T. Doutsos (1985). Quaternary tectonics in the Gulf of Patras, western Greece, Journal of Structural Geology, 7 (6), 713-717.

Fleury, J.J. (1980). Les zones de Gavrovo-Tripolitza et du Pinde-Olonos (Grèce continentale et Péloponnèse du Nord): evolution d'une plate-forme et d'un bassin dans leur carde alpin, Société Géologique du Nord, Special publication 4, 651 pp.

Fleury, J.J., P. De Wever, A. Izart and J. Dercourt (1981). Geological Map of Greece: Goumeron sheet, scale 1:50,000, IGME 1981, Athens.

Fountoulis, I., and E. Lekkas (1991). The occurrence of the Ionian Unit at Lapithas Mt. (Central-western Peloponnese, Greece). 1st Scientific Meeting of the Geological Society of Greece, May 1991, Xanthi, Bulletin of the Geological Society of Greece, 27, 47-56 (in Greek with English abstract).

Fountoulis, I., S. Mavroulis and D. Theocharis (2007a). The morphotectonic structure of the transitional zone between the Gortynia Mt. Horst and the Pyrgos_Olympia basin (Central-western Peloponnese, Greece), In: Proceedings of the 11th International Conference of the Geological Society of Greece (Athens, Greece, May 24-26, 2007), Bulletin of the Geological Society of Greece, 40 (1), 275-286.

Fountoulis, I., S. Mavroulis and D. Theocharis (2007b). Morphotectonic analysis and application of morphometric indices in the Lefkochori-Ochthia area (Central-western Peloponnese, Greece), In: Proceedings of the 8th Panhellenic Congress of the Geographical Society of Greece, 1, 198-208 (in Greek with English abstract).

Fountoulis, I., E. Vassilakis, S. Mavroulis, J. Alexopoulos and A. Erkeki (2011a). Quantification of river valley major diversion impact at Kyllini coastal area (W. Peloponnese, Greece) with remote sensing techniques, In: C. Grützner, R. Pérez-López, T. Fernández Steeger, I. Papanikolaou, K. Reicherter, P.G. Silva and A. Vött (eds.), Earthquake Geology and Archaeology: Science, Society and Critical facilities, Proceedings of the 2nd INQUA-IGCP 567 International Workshop on Active Tectonics, Earthquake Geology, Archaeology and Engineering (September 19-24, 2011, Corinth, Greece), 2, 42-45. ISBN:978-960-466-093-3.

Fountoulis, I., S. Mavroulis and E. Vassilakis (2011b). Shoreline displacement, drainage diversion in NW Peloponnese (Greece) as result of the geology, tectonics and human activity the last 100ky, In: Geomorphology 2011, 15th Joint Geomorphological meeting, Fluvial and coastal systems in tectonic active areas (Athens, Greece, June 1-4), book of abstracts.

Fountoulis, I., S. Mavroulis, E. Vassilakis and K. Papadopoulou-Vrynioti (2013). Shoreline displacement and Pineios River diversions in NW Peloponnese (Greece) as result of the geology, active tectonics and human activity during the last 100ky, Zeitschrift für Geomorphologie, 57, Suppl. 3, 97-123.

Galanopoulos, A.G. (1955). Seismic Geography of Greece, Annales Géologiques des Pays Hélléniques, 6, 83-121.

Galanopoulos, A.G. (1981). The earthquake potential of Greece, Annales Géologiques des Pays Hélléniques, 30, 648-724.

Ganas, A., E. Serpelloni, G. Drakatos, M. Kolligri, I. Adamis, Ch. Tsimi and E. Batsi (2009). The Mw 6.4 SW-Achaia (Western Greece) Earthquake of 8 June 2008: Seismological, Field, GPS Observations, and Stress Modeling, Journal of Earthquake Engineering, 13 (8), 1101-1124.

Gosar, A. (2012). Application of Environmental Seismic Intensity scale (ESI 2007) to Krn Mountains 1998 Mw=5.6 earthquake (NW Slovenia) with emphasis on rockfalls, Nat. Hazards Earth Syst. Sci., 12, 1659-1670.

Grünthal, G., ed. (1998). European Macroseismic Scale 1998 EMS-98, Conseil de l'Europe, Cahiers du Centre Européen de Géodynamique et de Séismologie, 15, Luxembourg.

Guerrieri, L., R. Tatevossian, E. Vittori, V. Comerci, E. Esposito, A.M. Michetti, S. Porfido and L. Serva (2007). Earthquake environmental effects (EEE) and intensity assessment: the INQUA scale project, Bollettino della Società Geologica Italiana, 126, 375-386.

Guerrieri, L., A.M. Blumetti, E. Esposito, A.M. Michetti, S. Porfido, L. Serva, E. Tondi and E. Vittori (2009). Capable faulting, environmental effects and seismic landscape in the area affected by the 1997 Umbria–Marche (Central Italy) seismic sequence, Tectonophysics, 476, 269-281.

Hageman, J. (1977). Stratigraphy and sedimentary History of the Upper Cenozoic of the Pyrgos area (W. Peloponnese, Greece), Annales Géologiques des Pays Hélléniques, 28, 299-333.

Hageman, J. (1979) Benthic foraminiferal assemblages from Plio-Pleistocene open bay to lagoonal sediments of the western Peloponnese (Greece), Utrecht Micropaleontological Bulletins, 20, 1-171.

Hancox, G.T., N.D. Perrin and G.D. Dellow (2002). Recent studies of historical earthquake-induced landsliding, ground damage, and MM intensity in New Zealand, Bulletin of the New Zealand Society for Earthquake Engineering, 35 (2), 59-95.

Hatzfeld, D., G. Pedotti, P. Hatzidimitriou, D. Panagiotopoulos, E. Scordilis, J. Drakopoulos, K. Makropoulos, N. Delibassis, J. Latoussakis, J. Baskoutas and M. Frogneux (1989). The Hellenic subduction beneath the Peloponnese: first results of a microearthquake study, Earth and Planetary Science Letters, 93, 283-291.

Hatzfeld, D., G. Pedotti, P. Hatzidimitriou and K. Makropoulos (1990). The strain pattern in the western Hellenic arc deduced from a microearthquake survey, Geophys. J. Int., 101, 181-202.

Hatzfeld, D., V. Karakostas, M. Ziazia, I. Kassaras, E. Papadimitriou, K. Makropoulos, N. Voulgaris and C. Papaioannou (2000). Microseismicity and faulting geometry in the Gulf of Corinth (Greece), Geophys. J. Int., 141, 438-456.

Kamberis, E., C. Alexiadis and P. Guy (1979). Geological Map of Greece: Amalias sheet, scale 1:50,000, IGME 1979, Athens.

Kamberis, E. (1987). Geology and petroleum geology study of NW Peloponnese, Greece, Ph.D. Thesis, National Technical University of Athens, Greece (in Greek).

Konstantinou K.I., N.S. Melis, S.-J. Lee, C.P. Evangelidis and K. Boukouras (2009). Rupture Process and Aftershocks Relocation of the 8 June 2008 Mw 6.4 Earthquake in Northwest Peloponnese, Western Greece, Bulletin of the Seismological Society of America, 99 (6), 3374-3389.

Kontopoulos, N., and T. Doutsos (1985). Sedimentology and tectonics of the Antirion area (Western Greece), Bollettino della Società Geologica Italiana, 104, 479-489.

Koukouvelas, I., A. Mpresiakas, E. Sokos and T. Doutsos (1996). The tectonic setting and earthquake ground hazards of the 1993 Pyrgos earthquake, Peloponnese, Greece. J. Geol. Soc., London, 153, 39-49.

Koukouvelas, I.K., S. Kokkalas and P. Xypolias (2010). Surface deformation during the Mw 6.4 (8 June 2008) Movri Mountain earthquake in the Peloponnese, and its implications for the seismotectonics of western Greece, International Geology Review, 52 (2-3), 249-268.

Kowalczyk, G., and K. Winter (1979). Outline of the Cenozoic history of the Kyllini peninsula, W. Peloponnese, In: N. Symeonides, D. Papanikolaou and M. Dermitzakis (eds.), Field Guide to the Neogene of Megara - Peloponnese - Zakynthos, Department of Geology and Paleontology, S.A. no. 34.

Lalechos, S., C. Metaxas, G. Papadopoulos and D. Fountoulis (2008). Earthquake Planning and Protection Organization Report: Aftershock sequence (09.06.2008 to 18.06.2008) of the June 8th, 2008 earthquake, Department of Seismotectonics, Earthquake Planning and Protection Organization.

Lekkas, E., E. Logos, G. Danamos, I. Fountoulis and E. Adamopoulou (1990). Macroseismic observations after the earthquake of October 16th, 1988 in Kyllini peninsula (NW Peloponnese, Greece), In: Proceedings of the 5th Geological Congress of the Geological Society of Greece (May 1990, Thessaloniki), Bulletin of the Geological Society of Greece, 25 (3), 313-328 (in Greek with English abstract).

Lekkas, E., D. Papanikolaou and I. Fountoulis (1992). Neotectonic Map of Greece, Sheets Pyrgos - Tropaia scale 1:100,000, Earthquake Planning & Protection Organization, 123 pp. (in Greek).

Lekkas, E., D. Papanikolaou, I. Fountoulis and G. Danamos. (1994) .Tectonic analysis of faults in the earthquake-affected area of Pyrgos. Scientific Applied Research Project, National and Kapodistrian University of Athens, Faculty of Geology, Department of Dynamic Tectonic Applied Geology, 35 pp.

Lekkas, E., D. Papanikolaou and I. Fountoulis (1995). The Pyrgos earthquake - The geological and geotechnical conditions of the Pyrgos area (W. Peloponnese, Greece), XV Congress of the Carpatho-Balcan Geological Association, Seminar on Active Faults, Geol. Soc. Greece, 42-46, Athens.

Lekkas, E., I. Fountoulis and D. Papanikolaou (2000). Intensity Distribution and Neotectonic Macrostructure Pyrgos earthquake data (26 March 1993, Greece), Natural Hazards, 21, 19-33.

Lekkas, E., G. Danamos and S. Lozios (2001). Neotectonic structure and evolution of Lefkada Island, In: Proceedings of the 9th Geological Congress of the Geological Society of Greece (September 2001, Athens), Bulletin of the Geological Society of Greece, 34 (1), 157-163 (in Greek with English abstract).

Lekkas, E., I. Fountoulis, G. Danamos, E. Skourtsos, L. Gouliotis, S. Mavroulis and I. Kostaki (2008a). Seismic fractures related to the NW Peloponnese (SW Greece) earthquake (ML=6.5R 8-6-2008), Preliminary Scientific Report, available at EERI http://www.eeri.org/site/images/lfe/pdf/greece_20080608_rpt1.pdf.

Lekkas, E., I. Fountoulis, G. Danamos, E. Skourtsos, L. Gouliotis, S. Mavroulis and I. Kostaki (2008b). Seismic Fractures Related to the NW Peloponnese (SW

Greece) Earthquake (ML=6.5R, 8-6-2008), 31st General Assembly of the European Seismological Commission, Crete, Abstract, 320.

Lekkas, E., I. Fountoulis, G. Danamos, E. Skourtsos, L. Gouliotis, I. Kostaki and S. Mavroulis, (2008c). Earthquake ML = 6.5R, 08.06.2008 Northwestern Peloponnese. Cross- Correlation of Seismic Intensities with Existing Seismotectonic, Geological, and Geotechnical Conditions, 31st General Assembly of the European Seismological Commission, Crete, Abstract, 239.

Margaris, B., Ch. Papaioannou, N. Theodoulidis, A. Savvaidis, N. Klimis, K. Makra, G. Athanasopoulos, G. Mylonakis and J. Stewart (2008). Preliminary Report on the Seismological and Geotechnical Engineering Aspects of the Mw=6.5 Achaia-Ilia (Greece) Earthquake on 8 June 2008, 31st General Assembly of the European Seismological Commission, Crete, Abstract, 239.

Margaris, B., G.A. Athanasopoulos, G. Mylonakis, C., Papaioannou, N. Klimis, N. Theodoulidis, A. Savvaidis, V. Efthymiadou and J.P. Stewart (2010). The 8 June 2008 Mw 6.5 Achaia-Elia, Greece earthquake: Source characteristics, ground motions, and ground failure, Earthquake Spectra, 26 (2), 399-424.

Mariolakos, I., D. Papanikolaou and E. Lagios (1985). A neotectonic geodynamic model of Peloponnese based on: morphotectonics, repeated gravity measurements and seismicity, Geol. Jb., 50, 3-17.

Mariolakos, I., and D. Papanikolaou (1987). Deformation pattern and relation between deformation and seismicity in the Hellenic arc, Bulletin of the Geological Society of Greece, 19, 59-76.

Mariolakos, I., E. Lekkas, G. Danamos, E. Logos and . Fountoulis (1989). Soil fractures and sand water's shaking off observed during the earthquake of October 16th, 1988 at the region of Vartholomio (W. Peloponnese, Greece), In: Proceedings of 1st Scient. Congress on Geophysics, Geophysist Club Greece, 535-563 (in Greek with English abstract).

Mariolakos, I., E. Lekkas, G. Danamos, E. Logos, I. Fountoulis and E. Adamopoulou (1990). Neotectonic evolution of the Kyllini Peninsula (NW Peloponnese), In: Proceedings of the 5th Congress (May 1990, Thessaloniki), Bulletin of the Geological Society of Greece, 25 (3), 163-176 (in Greek with Engish abstract).

Mariolakos, I., G. Danamos, I. Fountoulis, E. Lekkas and E. Logos (1991). Soil fractures and sand water's shaking off observed during the earthquake of October 16th, 1988 at the region of Vartholomio (W. Peloponnese, Greece), In: M.E. Almeida, R. Teixeira, R. Fantechi, R. Oliveira and A. Gomes Coelho (eds.), Proceedings of the European School of Climatology and Natural Hazards Course, Commis. Europ. Commun., EUR 12918 EN, Brussels, 257-265.

Mariolakos, I., I. Fountoulis and E. Lekkas (1995). The Neotectonics of NW Peloponnese - The earthquake of October 16, 1988, XV Congress of the Carpatho-Balcan Geological Association, Seminar on Active Faults, Geol. Soc. Greece, Athens, 33-41.

Mavroulis, S. (2009). Fault activity assessment in NW Peloponnese - The Andravida Earthquake (08/06/2008), MSc Thesis, Inter-University Post-Graduate Studies Programme on "Prevention and Management of Natural Disasters", Department of Geology and Geo-Environment of the National and Kapodistrian University of Athens, and Department of Geoinformatics and Topography of the Technological Educational Institute of Serres, 622 pp. (in Greek).

Mavroulis, S., I. Fountoulis and E. Lekkas (2010). Environmental effects caused by the Andravida (08-06-2008, ML=6.5, NW Peloponnese, Greece) earthquake, In: A. Williams, G. Pinches, C. Chin, T. McMorran and C. Massey (eds.), Geologically Active: 11th IAEG Congress, Taylor & Francis Group, Auckland, New Zealand, 451-459.

Melis, N.S., M. Brooks and R.G. Pearce (1989). A microearthquake study in the Gulf of Patras region, western Greece, and its seismorectonic interpretation, Geophys. J. R. Astr. Soc., 65, 741-762.

Mettos, A., and I. Karfakis (1991). Geological map of Greece: Evinohorion sheet, scale 1:50,000, IGME 1991, Athens.

Michetti, A.M., E. Esposito, A. Gurpinar, B. Mohammadioun, J. Mohammadioun, S. Porfido, E. Rogozhin, L. Serva, R. Tatevossian, E. Vittori, F. Audemard, V. Comerci, S. Marco, J. McCaplin and N.A. Morner (2004). The INQUA scale: an innovative approach for assessing earthquake intensities based on seismically induced ground effects in natural environment, Memorie descrittive della Carta Geologica d'Italia, Special Paper, 67, 118.

Michetti, A.M., E. Esposito, L. Guerrieri, S. Porfido, L. Serva, R. Tatevossian, E. Vittori, F. Audemard, T. Azuma, J. Clague, V. Comerci, A. Gürpinar, J. McCalpin, B. Mohammadioun, N. A. Mörner, Y. Ota and E. Roghozin (2007). Environmental Seismic Intensity Scale 2007 - ESI 2007, In: L. Guerrieri and E. Vittori (eds.), Memorie descrittive della Carta Geologica d'Italia, 74, 7-54.

Papadopoulos, G.A., V. Karastathis, C. Kontoes, M. Charalampakis, A. Fokaefs and I. Papoutsis (2010). Crustal deformation associated with east Mediterranean strike-slip earthquakes: The 8 June 2008 Movri (NW Peloponnese), Greece, earthquake (Mw

6.4), Tectonophysics, 492, 201-212.

Papanikolaou, D., I. Fountoulis and C. Metaxas (2007). Active faults, deformation rates and Quaternary paleogeography at Kyparissiakos Gulf (SW Greece) deduced from onshore and offshore data, Quaternary International, 171-172, 14-30.

Papanikolaou, I.D., and E.L. Lekkas (2008). Lithostratigraphic differentiation of the Gavrovo and the Ionian flysch in the Southern Akarnania and the role of the Agrilia and Evinos transverse fault zones, Hellenic Journal of Geosciences, 43, 41-55.

Papanikolaou, I.D., D.I., Papanikolaou and E.L. Lekkas (2009). Advances and limitations of the Environmental Seismic Intensity scale (ESI 2007) regarding near-field and far-field effects from recent earthquakes in Greece. Implications for the seismic hazard assessment, In: K. Reicherter, A.M. Michetti and P.G. Silva (eds.), Paleoseismology: Historical and Prehistorical Records of Earthquake Ground Effects for Seismic Hazard Assessment, Special Publication of the Geological Society of London, 316, 11-30.

Papanikolaou, I.D. (2011). Uncertainty in intensity assignment and attenuation relationships: How seismic hazard maps can benefit from the implementation of the Environmental Seismic Intensity scale (ESI 2007), Quaternary International, 242, 42-51.

Papathanassiou, G., S. Valkaniotis, A. Chatzipetros, P. Neofotistos, S. Sboras and S. Pavlides (2008). Liquefaction-induced ground disruption triggered by the earthquake of June 8, 2008 in NW Peloponnesus, Greece, In: Proc. of the 31st General Assembly of the European Seismological Commission ESC 2008 (Hersonissos, Crete, Greece, September 7-12, 2008).

Papazachos, B., and C. Papazachou (1997). The Earthquakes of Greece. Ziti Publications, Thessaloniki, Greece, 304.

Pavlides, S., S. Valkaniotis, G. Papathanassiou, S. Sboras and A. Chatzipetros (2008). Surface effects of the strong June 8, 2008, NW Peloponnese earthquake, In: 3rd National Conference on Earthquake Engineering and Engineering Seismology (November 5-7, 2008), Article 2110 (in Greek with English abstract).

Philippson, A. (1898). La téctonique de l'Egeide, Annales de Géographie, 112-141.

Philippson, A. (1959). Die Griechischen Landschaften, vol I-IV, Klostermann, Frankfurt.

Piper, D.J., and A. Panagos (1981). Growth patterns of the Acheloos and Evinos deltas, western Greece, Sediment. Geol., 28, 111-132.

Porfido, S., E. Esposito, L. Guerrieri, E. Vittori, G. Tranfaglia and R. Pece (2007). Seismically induced ground effects of the 1805, 1930 and 1980 earthquakes in the Southern Apennines, Italy, Bollettino della Società Geologica Italiana, 126, 333-346.

Reicherter, K., A. Michetti and P.G. Silva, eds. (2009). Palaeoseismology: Historical and Prehistorical Records of Earthquake Ground Effects for Seismic Hazard Assessment, Geological Society of London, Special Publications, London, U.K., 316, 55-71.

Renz, C. (1955). Die vorneogene Stratigraphic der normal sedimentaren Formationen Griechenlands, IGSR, Athen, 637 pp.

Richter, D., and I. Mariolakos (1975). Neue Beobachtungen an der Grenze Eozän-Kalk/Flysch im Bereich der massive Klokova und Varassova (Gavrovozone, Ätolia-Griechenland), Pract. Acad. Athens, 50, 377-390.

Roumelioti, Z., C. Benetatos, A. Kiratzi, G. Stavrakakis and N. Melis (2004). A study of the 2 December 2002 (M5.5) Vartholomio (western Peloponnese, Greece) earthquake and of its largest aftershocks, Tectonophysics, 387 (1-4), 65-79.

Sachpazi, M., A. Hirn, C. Clément, F. Haslinger, M. Laigle, E. Kissling, P. Charvis, Y. Hello, J.-C. Lépine, M. Sapine and J. Ansorge (2000). Western Hellenic subduction and Cephalonia transform: Local earthquakes and plate transport and strain, Tectonophysics, 319, 301-319.

Serva, L. (1994). Ground effects in the intensity scales, Terra Nova, 6, 414-416.

Serva, L., E. Esposito, L. Guerrieri, S. Porfido, E. Vittori and V. Comerci (2007). Environmental effects from five hystorical earthquakes in Southern Apennines (Italy) and macroseismic intensity assessment: Contribution to INQUA EEE Scale Project, Quaternary Int., 173-174, 30-44.

Silva, P.G., M.A. Rodríguez Pascua, R. Pérez-López, T. Bardaji, J. Lario, P. Alfaro, J.J. Martínez-Díaz, K. Reicherter, J. Giménez García, J. Giner, J.M. Azañón, J.L. Goy and C. Zazo (2008). Catalogacion de losefectos geologicos y ambientales de los terremotos en Espana en la Escala ESI 2007 y su aplicacion a losestudions paleosismologicos, Geotemas, 6, 1063-1066.

Stamatopulos, L., G. Belluomini, M. Branca, L. Manfra and M. Voltaggio (1988). $^{230}Th/^{234}U$ and isoleucine epimerization dating of Quaternary marine deposits in western Peloponnese (Greece), Z. Geomorph. N. F., 42 (2), 245-253.

Tsoflias, P. (1969). Geological structure of the northern part of Peloponnese (Achaia County), Annales Géologiques des Pays Hélléniques, 21, 554-651.

Tsoflias, P. (1977). Geological Map of Greece: Nea Manolas sheet, scale 1:50,000, IGME 1977, Athens.

Tsoflias, P. (1980). Geological Map of Greece: Patras sheet, scale 1:50,000, IGME 1980, Athens.

Tsoflias, P. (1984). Geological Map of Greece: Chalandritsa sheet, scale 1:50,000, IGME 1984, Athens.

Underhill, R. (1985). Neogene and Quaternary tectonics and sedimentation in Western Greece, PhD. thesis, University of Wales, Cardiff.

Underhill, R. (1988). Triassic evaporites and Plio-Quaternary diapirism in western Greece, Journal of the Geological Society, London, 145, 269-282.

Vassilakis, E., L. Royden and D. Papanikolaou (2006). Extensional neotectonic structures adjacent and sub-parallel to the Hellenic trench, Geological Society of America Abstracts with Programs, 38 (7), 549.

Vassilakis, E., L. Royden and D. Papanikolaou (2011). Kinematic links between subduction along the Hellenic trench and extension in the Gulf of Corinth, Greece: A multidisciplinary analysis, Earth Planet. Sci. Lett., 303, 108-120.

Wells, D.L., and K.J. Coppersmith (1994). New empirical relationships among magnitude, rupture length, rupture width, rupture area, and surface displacement, Bulletin of the Seismological Society of America, 84, 974-1002.

Winter, K.P. (1979). Zur neotektonischen Entwicklung im Bereich der Kyllini-Halbinsel (Vartholomion sheet), W. Peloponnes, In: G. Kallergis (ed.), Proceedings of the VI Colloquium on the Geology of the Aegean region, IGME, Greece, 1, 425-434.

*Corresponding author: Spyridon D. Mavroulis,
National and Kapodistrian University of Athens, Faculty of Geology and Geoenvironment, Department of Dynamic Tectonic Applied Geology, Panepistimiopolis, Athens, Greece;
email: smavroulis@geol.uoa.gr.